European Journal of Agronomy xxx (xxxx) 126744

Contents lists available at ScienceDirect

European Journal of Agronomy

journal homepage: www.elsevier.com/locate/eja

Quantifying critical N dilution curves across G × E × M effects for potato using a partially-pooled Bayesian hierarchical method

Brian J. Bohman [a,*], Michael J. Culshaw-Maurer [b], Feriel Ben Abdallah [c], Claudia Giletto [d], Gilles Bélanger [e], Fabián G. Fernández [a], Yuxin Miao [a], David J. Mulla [a], Carl J. Rosen [a]

[a] Department of Soil, Water, and Climate, University of Minnesota, 1991 Upper Buford Circle, St. Paul, MN 55108, USA
[b] CyVerse, University of Arizona, Tuscon, AZ, USA
[c] Productions in Agriculture Department, Crop Production Unit, Walloon Agricultural Research Centre (CRA-W), Gembloux, Belgium
[d] Unidad Integrada Balcarce, Facultad de Ciencias Agrarias (UNMdP)-INTA Balcarce, Ruta 226km 73,5, 7620 Balcarce, Buenos Aires, Argentina
[e] Science and Technology Branch, Agriculture and Agri-Food Canada, Québec, Canada

ARTICLE INFO

Keywords:
Critical N concentration
Critical nitrogen dilution curve
Nitrogen nutrition index
Nitrogen use efficiency
Potato
Bayesian
Genotype-by-environment-by-management interactions

ABSTRACT

Multiple critical N dilution curves [CNDCs] have been previously developed for potato; however, attempts to directly compare differences in CNDCs across genotype [G], environment [E], and management [M] interactions have been confounded by non-uniform statistical methods, biased experimental data, and lack of proper quantification of uncertainty in the critical N concentration [$\%N_c$]. This study implements a partially-pooled Bayesian hierarchical method to develop CNDCs for previously published and newly reported experimental data, systematically evaluates the difference in $\%N_c$ [$\Delta\%N_c$] across G × E × M effects, and directly compare CNDCs from the Bayesian framework to CNDCs from conventional statistical methods. The partially-pooled Bayesian hierarchical method implemented in this study has the advantage of being less susceptible to inferential bias at the level of individual G × E × M interactions compared to alternative statistical methods that result from insufficient quantity and quality of experimental datasets (e.g., unbalanced distribution of N limiting and non-N limiting observations). This method also allows for a direct statistical comparison of differences in $\%N_c$ across levels of the G × E × M interactions. Where found to be significant, $\Delta\%N_c$ was hypothesized to be related to variation in the timing of tuber initiation (e.g., maturity class) and the relative rate of tuber bulking (e.g., planting density) across G x E × M interactions. In addition to using the median value for $\%N_c$ (i.e., CNDC), the lower and upper boundary values for the credible region (i.e., $CNDC_{lo}$ and $CNDC_{up}$) derived using the Bayesian framework should be used in calculation of N nutrition index (and other calculations) to account for uncertainty in $\%N_c$. Overall, this study provides additional evidence that$\%N_c$ is dependent upon G × E × M interactions; therefore, evaluation of crop N status or N use efficiency must account for variation in $\%N_c$ across G × E × M interactions.

1. Introduction

Identifying optimal crop nitrogen [N] status to maximize growth and yield production is an elusive goal. Traditionally, either the yield-goal approach or rate-response curves have been used to identify optimal N fertilizer application rate (Morris et al., 2018). The N nutrition index [NNI] is an alternative approach to the current paradigm and comprises a well-developed framework to determine optimal crop N status (Lemaire et al., 2019). Typically, NNI is used to determine crop N status using whole plant analysis and to direct adaptive N management within a growing season (Houlès et al., 2007; Morier et al., 2015). The NNI framework has conventionally been considered generalizable

Abbreviations: NUE, nitrogen use efficiency; NUpE, nitrogen uptake efficiency; NUtE, nitrogen utilization efficiency; NNI, nitrogen nutrition index; CNDC, critical nitrogen dilution curve; CNUC, critical nitrogen uptake curve; CNUtEC, critical nitrogen utilization efficiency curve; W, total dry weight plant biomass; N_{Plant}, plant nitrogen content, $\%N_{Plant}$, plant nitrogen concentration; $\%N_c$, critical plant nitrogen concentration; $NUtE_c$, critical nitrogen utilization efficiency; $\Delta\%N_c$, difference in critical nitrogen concentration; $\%N_{c,\ up}$, upper bounds of credible interval for critical nitrogen concentration; $\%N_{c,\ lo}$, lower bounds of credible interval for critical nitrogen concentration; NNI_{up}, upper bound of credible interval for nitrogen nutrition index value; NNI_{lo}, lower bound of credible interval for nitrogen nutrition index value; $CNDC_{lo}$, lower boundary of credible region for critical nitrogen dilution curve; $CNDC_{up}$, upper boundary of credible region for critical nitrogen dilution curve; G, genotype; E, environment; M, management; EONR, economically optimum nitrogen rate

* Corresponding author.
E-mail address: bohm0072@umn.edu (B.J. Bohman).

https://doi.org/10.1016/j.eja.2023.126744
Received 27 June 2022; Received in revised form 4 January 2023; Accepted 9 January 2023
1161-0301/

across E × M effects (e.g., year-to-year, geographic, or cultural practices variability) and can be defined for any particular G effect (e.g., crop species or cultivar). In this manner, NNI reflects intrinsic physiological properties and reflects absolute crop N status across variation in environmental conditions (e.g., net soil N supply) or management practices (e.g., rate, source, timing, and placement of N fertilizer) (Sadras and Lemaire, 2014).

The NNI approach is defined based on the allometric relationship of declining plant N concentration [$\%N_{Plant}$] with increasing plant biomass, referred to as the critical N dilution curve [CNDC], which defines the critical N concentration [$\%N_c$] below which relative growth rate is reduced (Gastal et al., 2015):

$$\%N_c = aW^{-b} \quad (1)$$

where W represents dry weight plant biomass, and *a* and *b* are empirically fitted parameters. Parameter *a* is numerically equivalent to $\%N_c$ expressed in units of g N 100 g^{-1} when W is equal to 1 Mg ha^{-1}, and parameter *b* represents the ratio of the relative rate of decline in $\%N_c$ to the relative rate of increase in W. Using the CNDC, NNI values are then calculated as ratio of $\%N_{Plant}$ and $\%N_c$:

$$NNI = \%N_{Plant}/\%N_c \quad (2)$$

When NNI is greater than 1.0, crop N status is said to be in excess, and crop growth is not limited by N, while when NNI is less than 1.0, crop N status is deficient, and crop growth is limited by N. At NNI equal to 1.0, crop N status is optimal (Lemaire and Gastal, 1997).

A robust theoretical framework has been developed to explain decline in N concentration as biomass increases, but the application of this theory is most commonly restricted to the vegetative period where only metabolic and structural tissues are present (Greenwood et al., 1990; Justes et al., 1994; Sadras and Lemaire, 2014). Dilution of N in vegetative tissue occurs in relationship to an increasing proportion of structural biomass, with low N concentration, relative to metabolic (i.e., photosynthetic) biomass, with high N concentration (Lemaire and Gastal, 1997; Gastal et al., 2015).

Multiple previous studies have extended and empirically validated the CNDC relationships beyond its typical applications to describe declining N concentration over the entire crop growth cycle, including periods of reproductive growth, by including consideration of storage tissues in addition to structural and metabolic tissues (Greenwood et al., 1986; Duchenne et al., 1997; Plénet and Lemaire, 2000; Herrmann and Taube, 2004). Acceleration of N dilution beyond the vegetative period primarily occurs as low N biomass (i.e., starch) accumulates in storage tissues such as grain or tubers where the rate of decline is determined by the relative N concentration in storage biomass compared to vegetative biomass (Duchenne et al., 1997; Plénet and Lemaire, 2000). Duchenne et al., 1997 observed that as an increasing proportion of biomass accumulates in tubers, the rate of decline in N concentration increases with increasing biomass. Certain crops, such as potato, exclusively use a CNDC based on whole plant biomass due to the complex relationship between vine growth and tuber production (Duchenne et al., 1997; Bélanger et al., 2001a; Giletto and Echeverría, 2015; Ben Abdallah et al., 2016). Despite the validity of this approach, interpretating variation in CNDC observed between cultivars and geographies has been challenging.

However, recent work by Giletto et al. (2020) identified a mechanistic relationship underpinning the observed empirical relationships in N dilution for potato. The CNDC based on whole plant biomass reflects dilution in both the tuber and vine biomass, individually, and the increasing proportion of biomass allocated to low concentrations of N in biomass (i.e., tubers) as whole plant biomass increases. Giletto et al. (2020) also observed that varieties and locations with a greater proportion of biomass allocated to tubers have a greater value for parameter *b* of the CNDC, where parameter *b* of the CNDC represents the relative rate of decline in $\%N_c$ as biomass increases.

Based on this framework developed by Giletto et al. (2020), it is reasonable to expect that variation in CNDC for potato would occur due to variation in total biomass and harvest index (i.e., timing of tuber initiation, relative rate of tuber bulking) across G × E × M gradients. Understanding the effects of G × E × M interactions on crop N requirements and status is critical to improving agronomic outcomes and N use efficiency [NUE] within cropping systems (Lemaire and Ciampitti, 2020).

Previous CNDCs for potato have been developed with different statistical methods and limited quantification of their uncertainty (Duchenne et al., 1997; Bélanger et al., 2001a; Giletto and Echeverría, 2015; Ben Abdallah et al., 2016). This makes it difficult to ascertain whether observed differences in CNDCs result from underlying G × E × M effects, are confounded by the limitations of the statistical approach, or biased due to insufficient quantity or quality of experimental data (e.g., unbalanced distribution of N limiting and non-N limiting observations).

The conventional approach to fit a CNDC consists of a two-step process: first, the critical points from the relationship of $\%N_{Plant}$ as a function of biomass are selected using statistical criteria; second, a negative exponential curve is fit to the subset of critical points using nonlinear regression. There are two commonly used statistical approaches to identify critical points: (1) linear-plateau curve fit and (2) ANOVA and protected multiple comparison. Using a linear-plateau curve to derive critical points was originally suggested by Justes et al. (1994). This approach is rigorous and requires sufficient empirical data such that a linear-plateau curve can be identified (i.e., at least one N limiting and at least two non-N limiting data points) for each observation date. Therefore, this approach can be difficult or impossible to implement due to potential limitations of the experimental data used such as insufficient levels of N treatments (i.e., fewer than three treatment levels) or interactions between management practices and environmental conditions (i.e., all observations are either N limiting or non-N limiting). In contrast, many studies use methods similar to Ben Abdallah et al. (2016) where critical points are determined using a simplified statistical method. In this approach, ANOVA is first used to identify experimental dates where variation in biomass is statistically significant. Subsequently, a protected multiple comparisons analysis is used to identify which experimental treatments had the highest level of biomass – the treatment level with the significantly greatest level of biomass is then defined as the critical point. While this statistical method is more flexible to implement, it cannot resolve deficiencies in the underlying empirical data (e.g., insufficient level of N treatments, interactions with environmental conditions). Therefore, the critical points selected using the simplified method may be biased due to inherent deficiencies of the underlying experimental data used.

Novel statistical methods developed first by Makowski et al. (2020) provide a framework which allows for standardization in statistical approach and quantification of uncertainty for deriving in CNDCs which enables comparison of $\%N_c$ across G × E × M interactions. In short, this framework implements a hierarchical Bayesian model which simultaneously identifies critical points using the linear-plateau method (e.g., Justes et al., 1994) while fitting the negative exponential curve which defines $\%N_c$. The advantage of this method is that it fits the CNDC from the entire set of experimental data for a given G × E × M interaction level and removes the arbitrary intermediate step of separately identifying critical points. This approach has already been successfully used by Ciampitti et al. (2021), Yao et al. (2021), and Fernández et al. (2021) to evaluate differences in CNDCs across G × E × M interactions for maize, wheat, and tall fescue cropping systems, respectively. Through this single-step process, the Bayesian hierarchical method both eliminates the need to separately identify critical points and implements the theoretically preferred method (e.g., linear-plateau curve fit) to select critical points.

The Bayesian hierarchical method, however, remains subject to inferential bias due to both limited quantity and quality of experimental data (Fernández et al., 2021; Fernandez et al., 2022). With respect to quantity, having an insufficient number of observations from a limited number of experimental trials to derive an individual CNDC will result in increased bias in $\%N_c$. With respect to quality, using experimental data that does not reflect a full range of biomass values or does not sufficiently represent both limiting and non-limiting N conditions will result in increased bias in $\%N_c$. Datasets used to derive the CNDC using the Bayesian hierarchical method should contain at least eight experimental trials containing at least three N treatments and at least three sampling dates (Fernandez et al., 2022).

However, there are multiple approaches to pooling across G × E × M interactions within the Bayesian hierarchical method to address this bias due to experimental data limitations: no pooling, full pooling, and partial pooling. The no pooling approach treats each experimental data level independently where experimental data from one level is not used in inference for any other level (McElreath, 2020). The no pooling approach was used by Makowski et al. (2020), Ciampitti et al. (2021), Yao et al. (2021), and Fernández et al. (2021) to develop independent models for each G × E × M interaction. For the Bayesian hierarchical method, the no pooling approach is directly limited by the quantity and quality of experimental data for each G × E × M interaction level. The full pooling approach, in contrast, treats each experimental data level in an equivalent manner where the experimental data from all levels are used simultaneously for inference (McElreath, 2020). The full pooling approach was used by Fernández et al. (2021) to develop a single model across G × E × M interaction levels. While this approach was found by Fernández et al. (2021) to potentially reduced inferential bias from the Bayesian hierarchical method (i.e., by increasing the combined quantity and quality of data used to fit a given CNDC), the fully pooled approach has the explicit tradeoff that inference at individual levels of G × E × M interactions is not possible. The partial pooling approach balances the tradeoffs between fitting a single population-level model (i.e., full pooling) and fitting multiple independent group-level models (i.e., no pooling) by using the entire set of experimental data to fit a single model with where the data from all other levels of an effect influence the inference for a particular level and reduce inferential bias (McElreath, 2020). In this manner, individual effect levels are said to be "borrowing strength" through the process of "shrinkage", where more extreme values are pulled toward the average (Lindstrom and Bates, 1990; Bates, 2010). Therefore, using a partially-pooled Bayesian hierarchical method should reduce the inferential bias for a given G × E × M interaction level where the quantity and quality of experimental data are not otherwise sufficient and enable inference for each individual G × E × M interaction level. However, the partial pooling approach has not yet been implemented within in the Bayesian hierarchical method to derive CNDCs.

Building upon previous work, the objectives of this study are to 1) develop CNDCs using the hierarchical Bayesian framework for potato varieties in Minnesota (from both previously published and unpublished experimental data) and for potato varieties in Argentina (Giletto and Echeverría, 2015), Canada (Bélanger et al., 2001a), and Belgium (Ben Abdallah et al., 2016) (from previously published experimental data), 2) extend the implementation of the hierarchical Bayesian framework using a partial pooling approach to compare CNDCs across G × E x M interactions based on the uncertainty in $\%N_c$ and curve parameters *a* and *b*, 3) identify the optimal methods to determine uncertainty in $\%N_c$ for use in calculating NNI and other derivative metrics, and 4) compare CNDCs developed with the hierarchical Bayesian framework methods to previously published CNDCs for the same data with different statistical methods.

2. Materials and methods

2.1. Experimental Data

This study combines experimental data from both newly reported and previously published sources (Ben Abdallah et al., 2016; Giletto et al., 2020). The data used for analysis in this study are summarized in Table 1 and the relevant methods related to the experimental trials are reported below. All individual experimental observations used in this study are presented in the Supplemental Materials (Table S1).

2.1.1. Newly reported data – Minnesota

Six individual plot-scale field experiments were conducted over a total of eight years (MN-1: 1991–1992; MN-2: 2014–2015, MN-3: 2016, MN-4: 2018–2019, MN-5: 2019, MN-6: 2020) at the Sand Plain Research Farm [SPRF] in Becker, MN (45º 23′ N, 93º 53′ W). A summary of the treatments and sampling design for each experiment is presented in Table 2, and a summary of key experimental factors across G, E, and M effects are presented in Table 3.

A randomized complete block design with three or four replicates was used in each field experiment. All experiments evaluated at least three N rates (0 – 400 kg N ha^{-1}) for Russet Burbank potato [*Solanum tuberosum* (L.)], with some studies evaluating additional potato varieties (Table 2). Nitrogen fertilizer was applied using various source and timing regimes including polymer coated urea applied at planting and/or emergence, split-applied urea and urea-ammonium nitrate at emergence and/or post-emergence, ammonium nitrate at planting, emergence, and/or post-emergence. Experiments that evaluated multiple varieties had either a factorial design, or split-plot design with variety treatment as the whole-plot and N treatment as the split-plot. Plots in these studies were between 5.4 and 6.4 m wide (6 or 7 × 0.9 m rows) and 6.1 – 9.1 m long. Experiments were planted each year in late-April to early-May and were mechanically harvested in mid-September with vines terminated one to two weeks prior to harvest. Apart from experimental N and variety treatments, all management and cultural practices were managed by the staff at the SPRF in accordance with common practices for the region (Egel, 2017). Nutrients were applied based on soil samples and University recommendations (Franzen et al., 2018; Rosen, 2018), and supplemental irrigation was applied based on the University recommended checkbook method (Wright, 2002; Steele et al., 2010). Additional details on experimental procedures for these studies have been previously reported (Table 2).

Table 1
Summary of experimental data used in this study.

Study	Location	Variety	Site-Years	Sampling Dates	Samples
Present Study	Minnesota	Clearwater	2	10	30
		Dakota Russet	2	14	70
		Easton	2	14	70
		Russet Burbank	9	52	328
		Umatilla Russet	2	10	30
Giletto et al. (2020)	Argentina	Bannock Russet	3	13	52
		Gem Russet	4	18	72
		Innovator	4	18	72
		Markies Russet	2	9	36
		Umatilla Russet	3	14	56
	Canada	Russet Burbank	4	30	104
		Shepody	4	30	105
Ben Abdallah et al. (2016)	Belgium	Bintje	17	49	238
		Charlotte	7	24	114

Table 2
Summary of newly reported experimental small-plot trials in Minnesota, USA.

Experiment	Year	N trts.[a]	N rates [kg ha^{-1}]	Varieties	Sampling Dates	Reference
MN-1	1991	10	0, 135, 180, 225, 270	Russet Burbank	12 June, 24 June, 2 July, 16 July, 30 July, 13 Aug, 10 Sept.	Rosen et al. (1992); Rosen et al. (1993); Errebhi et al. (1998)
	1992	10	0, 135, 180, 225, 270	Russet Burbank	10 June, 25 June, 17 July, 5 Aug., 26 Aug., 15 Sept.	
MN-2	2014	5	135, 200, 270, 335, 400	Russet Burbank, Dakota Russet, Easton	30 June, 15 July, 24 July, 11 Aug., 26 Aug., 8 Sept., 15 Sept.	Sun (2017); Sun et al. (2019); Sun et al. (2020)
	2015	5	135, 200, 270, 335, 400	Russet Burbank, Dakota Russet, Easton	23 June, 7 July, 21 July, 4 Aug., 17 Aug., 1 Sept., 16 Sept.	
MN-3	2016	4	45, 180, 245, 335	Russet Burbank	28 June, 13 July, 26 July, 3 Aug., 10 Aug., 13 Sept.	Crants et al. (2017)
MN-4	2018	3	135, 270, 400	Russet Burbank, Clearwater, Umatilla Russet	26 June, 10 July, 18 July, 1 Aug., 13 Sept.	Gupta, 2019; Gupta et al. (2020); Li et al. (2021)
	2019	3	135, 270, 400	Russet Burbank, Clearwater, Umatilla Russet	26 June, 11 July, 24 July, 7 Aug, 16 Sept.	
MN-5	2019	8	45, 155, 245, 290, 335	Russet Burbank	25 June, 9 July, 23 July, 6 Aug, 21 Aug, 16 Sept	Bohman et al. (2020)
MN-6	2020	8	55, 155, 245, 270, 290, 335	Russet Burbank	24 June, 7 July, 22 July, 4 Aug, 16 Sept.	Rosen et al. (2021)

[a] Including N source, timing, and placement combinations occurring at an equivalent N rate

Samples of vine biomass were harvested immediately prior to mechanical termination for determination of fresh weight vine yield. Harvested tubers were mechanically sorted into weight classes and graded (1997), and fresh weight tuber yield was determined as the sum of all weight classes and tuber grades. Harvested biomass was oven dried at 60ºC to determine dry matter content of vines and tubers. Dry weight tuber and vine biomass was calculated as the product of fresh weight and dry matter content for each tissue respectively. Total N concentration of vines and tubers was determined from subsamples of plant tissues with either combustion analysis (Elementar Vario EL III, Elementar Americas Inc., Mt. Laurel, NJ) using standard methods (Horneck and Miller, 1998), or with the salicylic Kjeldahl method (Horwitz et al., 1970). Total N content of vines and tubers was calculated as the product of N concentration and dry weight biomass for each tissue respectively. Total plant N content [N_{Plant}] (kg N ha^{-1}) was calculated from the sum of tuber and vine N content. Total plant dry weight biomass [W] (Mg dry wt. ha^{-1}) was calculated from the sum of vine and tuber dry weight biomass. Plant N concentration [$\%N_{Plant}$] (g N 100 g^{-1} dry wt.) was calculated as the ratio of N_{Plant} to W.

Whole-plant samples were also regularly collected during the period of late-May to early-September (Table 2). Two to three plants were harvested from each plot on four to six dates each year with vines, roots, and tubers each measured separately. Dry weight biomass, N concentration, and N content for vines and tubers were determined for these in-season plant tissue samples using the methods described above. Calculations for W, N_{Plant}, and $\%N_{Plant}$ were the same as methods previously described above.

2.1.2. Previously published data – Belgium, Argentina, and Canada

Data reported in two previous studies, Giletto et al. (2020) and Ben Abdallah et al. (2016), were included in the analysis conducted for the present study. The data from Giletto et al. (2020) comprises two separate experimental data sets from small-plot experiments conducted in Balcarce in the province of Buenos Aires, Argentina (37º 45′ S; 58º 18′ W) (Giletto and Echeverría, 2015) and in the upper St. John River Valley of New Brunswick, Canada (47º 03′ N; 67º 45′ W) (Bélanger et al., 2000, 2001a, 2001b). All data from the Giletto et al. (2020) study used in the present analysis was included in this previous publication.

The data from Ben Abdallah et al. (2016) represents multiple experimental data set from small-plot experiments were conducted in Gembloux, Belgium (50º 33′ N; 4º 43′ E). Only a portion of the data from the Ben Abdallah et al. (2016) study used in the present analysis was included in this previous publication – while the dry weight biomass data were previously reported, the N concentration data from the Ben Abdallah et al. (2016) experiment is reported for the first time in this work.

A summary of experimental data from each trial used in the present study is presented in Table 1, and a summary of key experimental factors across G, E, and M effects is presented in Table 3.

2.2. Statistical methods

Based on the general approach outlined by Makowski et al. (2020), this study implemented a partially-pooled Bayesian hierarchical framework to infer CNDC parameters for each location and variety within location, assess the uncertainty in model parameters and $\%N_c$, and compare fitted CNDCs across the effects of location and variety.

The Bayesian hierarchical framework outlined by Makowski et al. (2020) was extended to explicitly include the G × E × M interaction levels within the fitted model using a partial pooling approach. Experimental data were nested according to location and variety within location, where the linear-plateau curve fitted for each experimental sampling date is nested within a given level of variety within location (Fig. 1). This model structure leverages the advantages of partial pooling to addresses the limitations identified by Fernández et al. (2021) that a sufficient quantity and quality of experimental data are required while still enabling direct inference on the individual G × E × M interaction levels. Using *R* (R Core Team, 2021a), the *brms* package (Bürkner, 2017, 2018) was used to implement the statistical framework outlined by Makowski et al. (2020) with the modifications as previously described (Fig. 1). The *brms* package, an interface to *Stan* (Carpenter et al., 2017), was chosen due to the ability to include group-level effects (i.e., random effects) which allows for the fit of this particular partially-pooled Bayesian hierarchical model. The *brms* package includes a user-friendly modeling language, robust documentation, and a diverse set of tools to analyze and assess models.

A non-linear *brms* model was defined by combining the two separate expressions used by Makowski et al. (2020) to parameterize the Bayesian hierarchical model as previously implemented with *rjags* (Plummer, 2019) and *JAGS* statistical software (Plummer, 2013).

The first expression from Makowski et al. (2020) represents the linear-plateau component:

Table 3
Comparison of key experimental factors including for Genotype [G]: variety maturity class [Maturity Class]; Environment [E]: soil texture classification [Soil Texture], dates of typical growing season [Growing Season], soil organic matter content [OM], growing season mean daily temperature [T_{Mean}], growing season cumulative precipitation [Precip.], growing season mean diurnal temperature difference [$\Delta T_{Diurnal}$] calculated as the average of daily diurnal temperature difference (i.e., difference between daily max temperature and daily minimum temperature), growing season cumulative growing degree days [GDD] calculated with base temperature of 7 ºC and maximum temperature of 30 ºC, growing season mean daily incident solar radiation [Sol. Rad.]; and Management [M]: planting density [Density], N fertilizer application source and timing [N Source & Timing], and use of supplemental irrigation [Irr.].

		G	E								M		
Location	Variety	Maturity Class[a]	Soil Texture[b]	OM [%]	Growing Season[c]	T_{Mean} [ºC]	Precip. [mm]	$\Delta T_{Diurnal}$ [ºC]	GDD [ºC d]	Sol. Rad. [MJ m^{-b}]	Density [plants ha^{-a}]	N Source & Timing[d]	Irr.
Argentina	Bannock Russet	L to VL	L	4.2 – 5.2	1 June – 10 Oct.	18.4	428	13.6	1739	25.5	59,000	Urea @ PL	Yes
	Gem Russet	M to L											
	Innovator	E to M											
	Markies Russet	L to VL											
	Umatilla Russet	ML to L											
Belgium	Bintje	L	SiCL, SiL, L, SL	1.3 – 2.6	10 Oct. – 10 Mar.	15.5	244	8.3	1313	20.0	38,000	AN @ PL	No
	Charlotte	M											
Canada	Russet Burbank	L to VL	CL, L	2.6 – 3.0	20 Apr – 20 Sept.	15.7	371	10.0	1150	19.1	29,000	AN @ PL	Yes
	Shepody	E to ME									44,000		
Minnesota	Clearwater	ML	LS	1.3 – 2.5	1 May – 15 Sept.	18.9	383	11.6	1638	22.7	36,000[e]	AN, Urea, UAN, and/or PCU @ PL, EM, and/or P-EM	Yes
	Dakota Russet	ML											
	Easton	L											
	Russet Burbank	L to VL											
	Umatilla Russet	ML to L											

[a] Early [E], medium-early [ME], medium [M], medium-late [ML], late [L], very late [VL] as classified by Stark et al. (2020), Anon (2021), Giletto and Echeverría (2015), Anon (2013), Anon (2015), Thompson (2013), and Porter (2014)
[b] Silty clay loam [SiCL], clay loam [CL], silt loam [SiL], loam [L], sandy loam [SL], loamy sand [LS]
[c] Summary weather data based on typical growing season dates and historical climate reconstruction for the period of 1980–2016 (Gelaro et al., 2017; Anon, 2021)
[d] Ammonium nitrate [AN], urea-ammonium nitrate [UAN], polymer-coated urea [PCU], planting [PL], emergence [EM], post-emergence [P-EM]
[e] Russet Burbank in MN-1 was planted at a density of 48,000 plants ha^{-1}

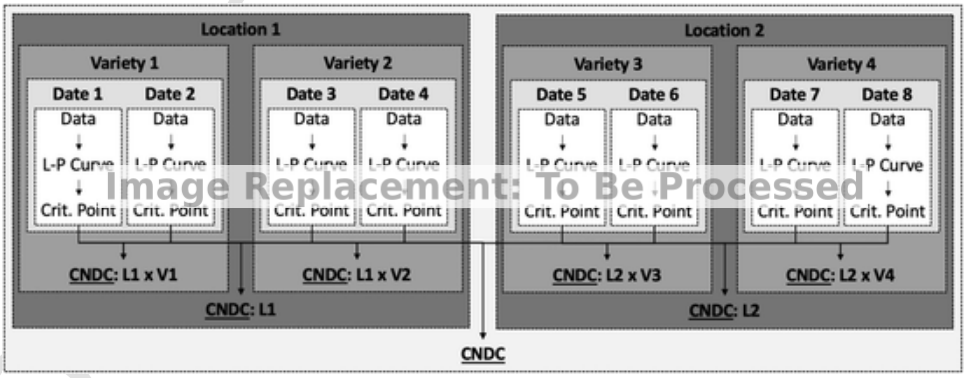

Fig. 1. Flowchart showing nested structure used to fit critical N dilution curves [CNDC] using the hierarchical Bayesian method based on Makowski et al. (2020). Linear-plateau (L-P) curves and critical points (i.e., the fitted join point of each linear-plateau curve) are identified at the level of each experimental sampling date and pooled at various levels of location and variety within location to determine the CNDC for that level. This hierarchical model structure simultaneously fits all individual levels of location and variety within location, as well as for the global level of all experimental data, which allows for direct comparison across levels.

$$W = \min\left(W_{Max,i} + S_i \times \left(\%N_{Plant} - \%N_c\right), W_{Max,i}\right) \quad (3)$$

where S_i and $W_{Max,i}$ are the slope of the linear-plateau curve and the maximum value of biomass (i.e., plateau) for a given date [i], respectively, *min* represents the minima function (i.e., the plateau component), and W, $\%N_{Plant}$, and $\%N_c$ have the same meaning as previously defined in this present study. This linear-plateau curve is defined with N concentration as the independent variable and biomass as the dependent variable and is written in point-slope form where the reference point used is the critical point.

The second expression from Makowski et al. (2020) represents the CNDC component:

$$\%N_c = aW_{Max,i}^{-b} \quad (4)$$

where *a* and *b* are the parameters that define the negative exponential curve and $\%N_c$ and $W_{Max,i}$ have the same meanings as defined above.

Using algebraic substitution (i.e., for $\%N_c$), these two expressions (Eq. (3) and Eq. (4)) were combined to produce following non-linear *brms* model formula:

$$W \sim min\left(W_{Max,i} + S_i\left(\%N_{Plant} - \left(aW_{Max,i}^{-b}\right)\right), W_{Max,i}\right) \quad (5)$$

Two group-level (i.e., random) effects were specified for this *brms* model to parameterize the nested structure (Fig. 1). First, the parameters S and W_{Max} included group-level effects to fit a linear-plateau curve to each experimental sampling date:

$$W_{Max} + S \sim 1 + (1|index) \quad (6)$$

where *index* represents the unique level of each experimental sampling date, nested within a given level of variety within location. Second, the parameters a and b included group-level effects to fit the CNDC:

$$a + b \sim 1 + (1|location) + (1|location:variety) \quad (7)$$

where *location* and *location:variety* represents the unique effect level for location and variety within location, respectively. Models were fit using treatment-level means (i.e., an effect of *replicate* was not included in the model).

The *brms* model was fitted using 4 chains and 10000 iterations with 3000 warmups per chain. Model convergence was verified by determining that all parameters had satisfactory R-hat values of less than 1.01 with bulk-ESS and tail-ESS values of at least 100 samples per chain (Vehtari et al., 2021). The priors for this model were chosen based on expert knowledge (i.e., previously reported values), empirical observations (i.e., summary values from the data set), and inspection of the joint prior predictive distribution. Evaluating the joint prior predictive distribution is particularly important for hyperparameters dealing with the standard deviation between groups in a hierarchical model due to the propagation of variance throughout model levels. If a set of relatively uninformative priors led to biologically or physically impossible predictions which prevented model convergence, the prior ranges were narrowed (Schad et al., 2021). In particular, a positive value for S is required to represent the positive physiological relationship between W and $\%N_{Plant}$ (i.e., linear-plateau curve where W increases as $\%N_{Plant}$ up to W_{max} at$\%N_c$). Similarly, having non-positive value for W_{max} is physically impossible. A summary of the prior values used in this model is given below (Table 4).

The entire statistical and data workflow used to generate this analysis is reproducible and available via GitHub repository (https://github.com/bohm0072/bayesian-cndc-potato). The *renv* package (Ushey, 2021) was used to document the computing environment utilized while conducting this analysis to ensure code portability and reproducibility.

Table 4
Priors used in fitting the hierarchical Bayesian model with *brms*.

Parameter	Distribution	Bounds	
		Lower	Upper
a	Normal (5.3, 0.1)	0	∞
$\sigma(a_{location})$	Normal (0.10, 0.02)	−∞	∞
$\sigma(a_{location:variety})$	Normal (0.05, 0.01)	−∞	∞
b	Normal (0.40, 0.01)	0	1
$\sigma(b_{location})$	Normal (0.05, 0.02)	−∞	∞
$\sigma(b_{location:variety})$	Normal (0.02, 0.01)	−∞	∞
W_{max}	Normal (8.0, 0.1)	1	∞
$\sigma(W_{max,index})$	Normal (7.0, 1.0)	−∞	∞
S	Normal (6.0, 0.1)	0	∞
$\sigma(S_{index})$	Normal (1.0, 0.1)	−∞	∞
σ	Student's t (3, 1.0, 0.1)	−∞	∞

2.3. Evaluating uncertainty

2.3.1. Critical N dilution curve parameter uncertainty

After the statistical model was successfully fit to the data (n = 28,000 draws), values for parameters a and b of the CNDC were reported at the 0.05, 0.50 (i.e., median) and 0.95 quantiles for the effect levels of *location* and *location:variety* to determine the 90% credible interval for each parameter. The correlation between values for parameters a and b was determined for each effect level of *location:variety* using the fitted parameter values at the level of the individual draws.

2.3.2. Critical N concentration uncertainty

Uncertainty in $\%N_c$ was characterized using three methods: (1) directly modeled 0.05 and 0.95 quantile value of posterior distribution of $\%N_c$; (2) parameterized approximation of 0.05 and 0.95 quantile value of posterior distribution of $\%N_c$; (3) indirect calculation of $\%N_c$ using 0.05 and 0.95 quantile values for a and b.

For the directly modeled method, $\%N_c$ for a set of discrete values of W between 1 Mg dry wt. ha^{-1} and the maximum observed value of W in the experimental data set was calculated for each individual posterior draw based on the fitted values of parameters a and b for that draw. From the distribution of $\%N_c$ values, the 0.05, 0.50 (i.e., median) and 0.95 quantile values were identified for each effect level of *location:variety* to determine the 90% credible region for $\%N_c$. This approach makes maximal use of the jointly estimated parameters contained in the posterior distribution.

For the parameterized approximation method, two negative exponential curve of the same form as the CNDC (i.e., $y = a\,x^{-b}$) were fit using *nls* (R Core Team, 2021b) to the 0.05 and 0.95 quantile values of the posterior distribution of $\%N_c$ computed using the directly modeled method described above. This approach to derive parameterized approximation of the 90% credible region attempts to simplify the complexity of communicating and propagating uncertainty in $\%N_c$. These parameterized curves approximating the upper and lower boundaries of the credible region for the CNDC are respectively referred to as $CNDC_{up}$ and $CNDC_{lo}$, where parameters a_{up} and b_{up} correspond to $CNDC_{up}$ and parameters a_{lo} and b_{lo} correspond to $CNDC_{lo}$:

$$\%N_{c,lo} = a_{lo}W^{-b\_lo} \quad (8)$$

$$\%N_{c,up} = a_{up}W^{-b\_up} \quad (9)$$

For the indirect calculation method, an estimate of the 90% credible region for $\%N_c$ was calculated by using the boundary values of the 90% credible interval of parameters a and b. The estimate for the upper boundary of the credible region for $\%N_c$ was determined from the 0.95 quantile value for parameter a and 0.05 quantile value for parameter b; the estimate for the lower boundary of the credible region of $\%N_c$ was determined from the 0.05 quantile value for parameter a and 0.95 quantile value for parameter b. This approach does not account for the joint estimation of parameters offered by the Bayesian approach; therefore, the paired combination for parameters a and b (i.e., 0.05 and 0.95 quantiles, respectively) might not actually occur in the posterior distribution.

Difference in critical N concentration [$\Delta\%N_c$] were calculated as the difference between a reference value [$\%N_{c,ref}$] and a comparison value [$\%N_{c,i}$]:

$$\Delta\%N_c = \%N_{c,ref} - \%N_{c,i} \quad (10)$$

To compare differences between the various methods used to quantify uncertainty in $\%N_c$, $\Delta\%N_c$ was calculated (Eq. (10)) where $\%N_{c,ref}$ was set as the median value (i.e., 0.50 quantile) of $\%N_c$ from the di-

rectly modeled method, while $\%N_{c,i}$ was varied and set as the upper and lower values of $\%N_c$ from the directly modeled, parameterized approximation, and indirect calculation methods as described above.

2.3.3. Comparing critical N concentration across G × E × M effects

Using the directly modeled method described above, $\%N_c$ for each posterior draw was calculated. At the effect level of *location:variety*, $\Delta\%N_c$ was calculated (Eq. (10)) where $\%N_{c,ref}$ is the median $\%N_c$ from the posterior distribution for the reference level and $\%N_{c,i}$ was the median $\%N_c$ from the posterior distribution for each pairwise comparison of all other levels. From this computed set of $\Delta\%N_c$, the 0.05, 0.50 (i.e., median) and 0.95 quantile values were identified for each pairwise comparison of *location:variety* levels to determine the 90% credible region for $\Delta\%N_c$. The comparison curve was considered to be not significantly different from the reference curve when the 90% credible region for $\Delta\%N_c$ contained zero. This approach allows for the direct evaluation of differences in $\%N_c$ across G × E × M effects (i.e., *location:variety* levels).

2.3.4. Comparing critical N concentration across statistical methods

An analogous method was also used to compare the CNDCs fitted in the present study to the CNDCs published in previous studies (i.e., Ben Abdallah et al., 2016; Giletto et al., 2020). Specifically, $\Delta\%N_c$ for each level of *location:variety* with previously published CNDC was calculated (Eq. (10)) using where $\%N_{c,ref}$ was set as the median value (i.e., 0.50 quantile) of $\%N_c$ from the directly modeled method, and $\%N_{c,i}$ was set as the previously published values of $\%N_c$. If $\Delta\%N_c$ falls outside of the 90% credible region for $\%N_c$ determined from the directly modeled method, then the two curves are determined to be significantly different over the range for which the previous value falls outside of the credible region. This approach allows for direct evaluation of differences in $\%N_c$ for CNDCs developed from the same set of data across various statistical methods.

3. Results

3.1. Fitted critical N dilution curve

The posterior distribution of fitted values for CNDC parameters *a* and *b* are presented in Fig. 2 showing the median value and 90% credible interval (i.e., 0.05 and 0.95 quantile values). For parameter *a*, there was no significant difference for the effect of location at 90% credible interval threshold (Fig. 2a). Although Argentina has a numerically greater value of parameter *a* (4.95) than the other three locations (4.74 – 4.77), these differences are not significant. Additionally, the variation in parameter *a* for the variety within location effect is negligible and not statistically significant (Fig. 2a).

For parameter *b*, there were significant differences for both the effect of location and variety within location at a 90% credible interval threshold (Fig. 2b). For location, Argentina had the lowest value for parameter *b* (0.175), while Canada had a greater value for parameter *b* (0.448) than Argentina but lower than either Belgium (0.561) or Minnesota (0.582). The difference between parameter *b* for Belgium and Minnesota was not significant. For the variety within location effect, parameter *b* significantly varied for varieties in Argentina and Canada, while there were no significant differences in parameter *b* within either Belgium or Minnesota. For Argentina, Innovator had the greatest value for parameter *b* (0.212), followed by Gem Russet, Umatilla Russet,

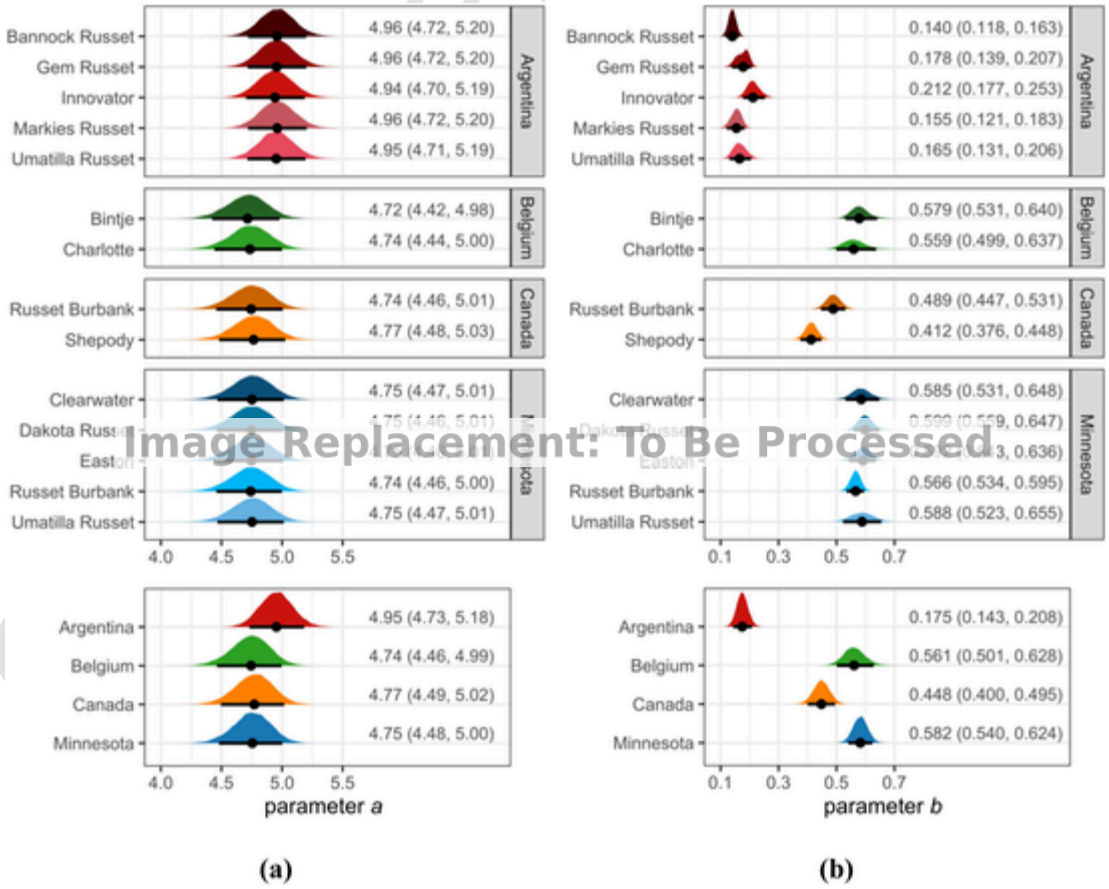

Fig. 2. Posterior distribution of variety and variety within location effects for (a) parameter *a*; and (b) parameter *b*. Points represent median value and line represents 0.05 and 0.95 quantile range. Values displayed with the figures are the median value with the 90% credible interval boundaries (i.e., 0.05 and 0.95 quantiles) displayed within the parentheses.

Markies Russet, and Bannock Russet (0.178, 0.165, 0.155, and 0.140, respectively). The difference between Innovator and Umatilla Russet, Markies Russet, and Bannock Russet was significant, while all other differences between varieties were not significant. For Canada, Russet Burbank had a significantly higher value for parameter *b* (0.489) than Shepody (0.412).

There was a positive correlation found between parameters *a* and *b* (Fig. 3) which indicates that quantifying differences in these parameter values independently (Fig. 2) is not appropriate to describe the uncertainty in $\%N_c$ determined by the correlated parameters. Stated alternatively, significant differences for either parameter *a* or *b* do not necessarily imply that differences in $\%N_c$ are also significant.

Critical N dilution curves for each variety within location and the experimental data, median linear-plateau curve for each experimental sampling date, and median value of $\%N_c$ are presented (Fig. 4). The individual linear-plateau curves fitted for each experimental sampling date nested within each level of the variety within location effect are presented in the Supplemental Materials (Fig. S1).

For the Argentina varieties, more than 60% of the observed data fall below the CNDC (i.e., represent N limiting conditions) with over 40% of sampling dates having exclusively N limiting conditions observed. For both the Belgium and Minnesota varieties, more than 80% of the observed data fall above the CNDC (i.e., represent non-N limiting conditions) with almost 30% of sampling dates having exclusively non-N limiting conditions observed. For the Canada varieties, over 60% of observed data represented non-N limiting conditions but less than 10% of sampling dates had exclusively non-N limiting conditions observed (Fig. S1).

3.2. Critical N concentration uncertainty

The credible region for $\%N_c$ varies across variety within location and across levels of biomass (Fig. 5). The symmetry of the credible region distribution varies by variety within location. Some levels of variety within location, such as Argentina × Gem Russet, have a skewed distribution, while other levels, such as Canada × Shepody, have a symmetrical distribution (Fig. 5a). There are also differences in the range of the credible region, where some varieties within location, such as Argentina × Umatilla Russet, have greater uncertainty in $\%N_c$ than others, such as Minnesota × Russet Burbank. The uncertainty in $\%N_c$ also varies across the level of biomass for a given CNDC. For example, as the level of biomass increases, Argentina × Umatilla Russet has an increasing credible region range, Minnesota × Russet Burbank has a decreasing credible region range, and Argentina × Bannock Russet has a nearly constant credible region range.

Estimation of the upper and lower boundaries of the 90% credible region using the parameterized estimate approach (i.e., $CNDC_{lo}$ and $CNDC_{up}$) (Table 5) appears to be reasonable based on graphical evaluation (Fig. 5). However, these fitted $CNDC_{lo}$ and $CNDC_{up}$ curves do not themselves represent a draw directly from the posterior distribution and do not necessarily represent the most extreme possible curves. While credible regions with boundaries that are non-monotonic (e.g., Argentina × Innovator) have portions of the curve fit approximation that are poorer performing, the credible regions with monotonic boundaries (e.g., Minnesota × Dakota Russet) seem to be satisfactory across the entire range of the curve.

However, the approximation of uncertainty in $\%N_c$ based on the indirect calculation method were found to contain the entire credible region for all varieties within location evaluated (Fig. 5). Therefore, the indirect calculation approach based on uncertainty in CNDC parameters is less informative than either the directly modeled or parameterized estimate approaches. In the absence of the credible region defined directly from the fitted hierarchical Bayesian model (i.e., directly modeled approach), using the $CNDC_{lo}$ and $CNDC_{up}$ (Table 5) (i.e., parameterized estimate approach) is a suitable first-order representation of the credible region for $\%N_c$.

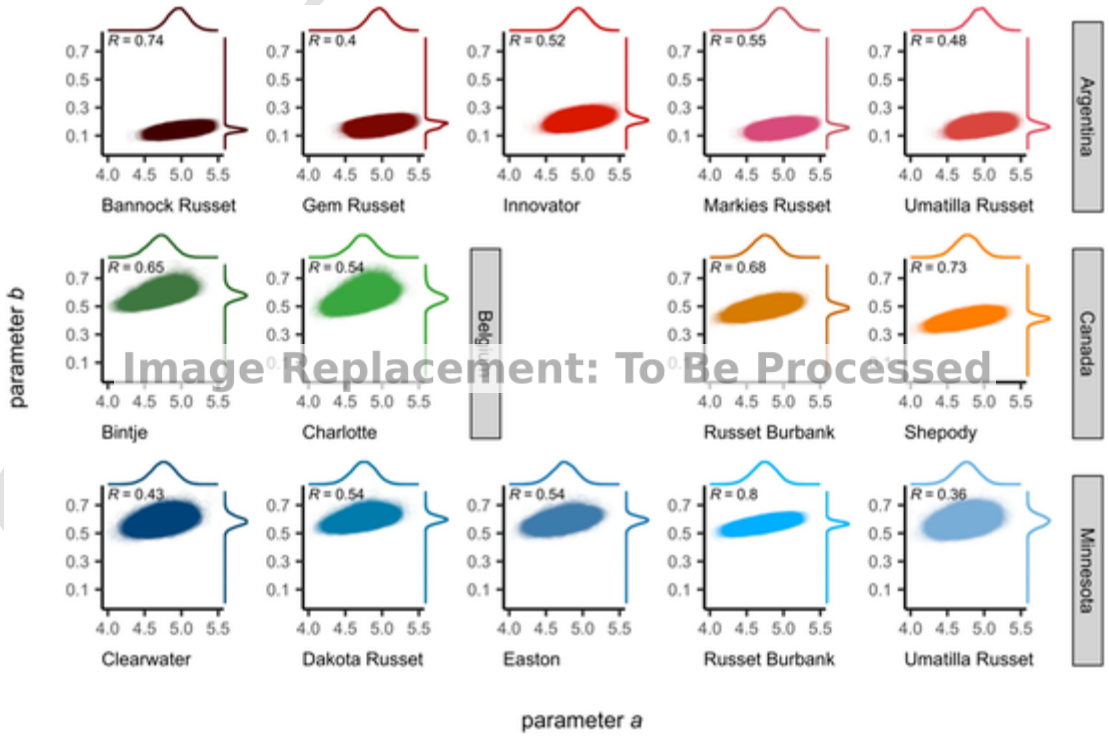

Fig. 3. Distribution of posterior values for parameters *a* and *b* for each location within variety shown as a scatterplot with marginal density distribution given for each parameter. Pearson correlation coefficient [*R*] is displayed for the relationship between parameters *a* and *b*. Data are shown at the level of individual draws (n = 28,000).

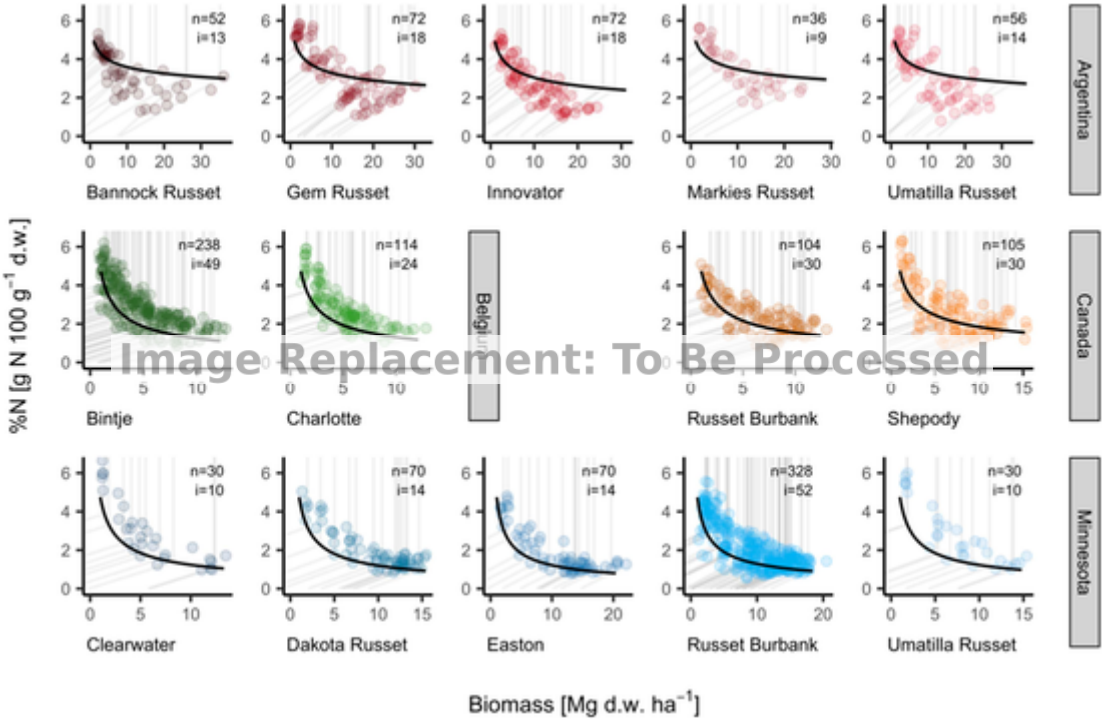

Fig. 4. Critical N dilution curves (i.e., median value of critical N concentration [$\%N_c$]) fitted from the hierarchical Bayesian model are shown as a solid black lines for each variety within location. Biomass and N concentration [%N] data are displayed as points with the median linear-plateau curve for each sampling date shown as grey line. The number of samples [n] and the number of sampling dates [i] are displayed on each individual panel.

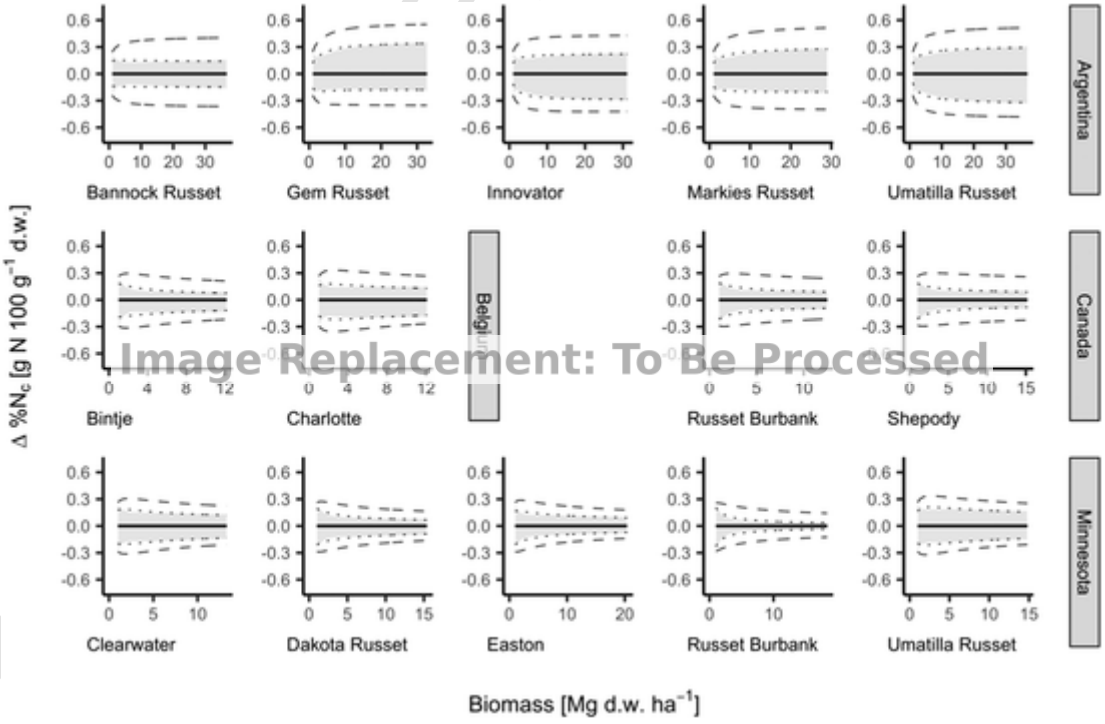

Fig. 5. Comparison of the difference in critical N concentration values [$\Delta\%N_c$]. The reference critical N concentration [$\%N_{c,ref}$] is represented as a solid black line at constant $\Delta\%N_c$ value of zero. The grey shaded region represents the 90% credible region of $\%N_c$ from the directly modeled approach (i.e., $\%N_c$ computed from parameter estimates of each posterior draw). The dotted lines represent the estimated upper and lower bounds of $\%N_c$ from the parameterized estimate approach (i.e., $CNDC_{lo}$ and $CNDC_{up}$). The dashed lines represent the approximated lower and upper bounds of $\%N_c$ from the indirect calculation approach (i.e., $\%N_c$ computed based on posterior distribution of parameters *a* and *b*). Data are presented for all levels of variety within location.

Table 5
Critical N dilution curve parameters for each variety within location, with the median value of the posterior distribution for parameters *a* and *b* (CNDC), and the estimates for the credible region lower ($CNDC_{lo}$) and upper ($CNDC_{up}$) boundaries using the parameterized estimate approach.

Location	Variety	$CNDC_{lo}$		CNDC		$CNDC_{up}$	
		a_{lo}	b_{lo}	a	b	a_{up}	b_{up}
Argentina	Bannock Russet	4.82	0.146	4.96	0.140	5.10	0.135
	Gem Russet	4.80	0.190	4.96	0.178	5.07	0.152
	Innovator	4.83	0.241	4.94	0.212	5.06	0.193
	Markies Russet	4.82	0.167	4.96	0.155	5.08	0.135
	Umatilla Russet	4.85	0.195	4.95	0.165	5.06	0.143
Belgium	Bintje	4.52	0.606	4.72	0.579	4.90	0.567
	Charlotte	4.56	0.607	4.74	0.559	4.89	0.531
Canada	Russet Burbank	4.53	0.498	4.74	0.489	4.93	0.480
	Shepody	4.55	0.416	4.77	0.412	4.95	0.406
Minnesota	Clearwater	4.56	0.622	4.75	0.585	4.93	0.558
	Dakota Russet	4.54	0.619	4.75	0.599	4.94	0.588
	Easton	4.54	0.608	4.75	0.592	4.91	0.567
	Russet Burbank	4.51	0.562	4.74	0.566	4.95	0.567
	Umatilla Russet	4.56	0.631	4.75	0.588	4.92	0.546

3.3. Evaluating differences between critical N concentration

3.3.1. Differences related to G × E × M effects

While an evaluation of the pairwise differences between all varieties within location was conducted and is presented in the Supplemental Materials (Fig. S2), a subset of the results comparing Minnesota × Russet Burbank to all other varieties within location, Argentina × Innovator to all other varieties within Argentina, Canada × Russet Burbank to all other varieties within Canada, and Belgium × Bintje to all other varieties within Belgium are presented in detail here (Fig. 6).

For Minnesota × Russet Burbank, there were no significant differences in $\%N_c$ for any level of W evaluated with any of the other varieties in Minnesota (i.e., Clearwater, Dakota Russet, Easton, and Umatilla Russet) or with the Belgium varieties (i.e., Bintje, and Charlotte) (Fig. 6a). The $\%N_c$ values for both of the Canadian varieties (i.e., Russet Burbank, and Shepody) were significantly greater than that for Minnesota × Russet Burbank when biomass values were greater than 2 Mg ha^{-1} dry wt. The $\%N_c$ for Canada × Russet Burbank and Canada × Shepody were up to 0.3 and 0.6 g N 100 g^{-1} dry wt. greater than that for Minnesota × Russet Burbank, respectively. The $\%N_c$ for the Argentina varieties (i.e., Bannock Russet, Gem Russet, Innovator, Markies Russet, and Umatilla Russet) were significantly greater than for Minnesota × Russet Burbank, except at a biomass value of 1.0 Mg dry wt. ha^{-1}, with a difference in value depending on variety of up to 2.4 g N 100 g^{-1} dry wt.

For Argentina × Innovator, $\%N_c$ was significantly lower than for Argentina × Bannock Russet, Argentina × Markies Russet, and Argentina × Umatilla Russet but was not significantly different from Argentina × Gem Russet (Fig. 6b). The $\%N_c$ values for Argentina × Bannock Russet, Argentina × Markies Russet, and Argentina × Umatilla Russet were up to 0.5 g N 100 g^{-1} dry wt. greater than that for Argentina × Innovator. For Canada × Russet Burbank, $\%N_c$ was significantly lower than for Canada × Shepody (Fig. 6c), with a difference in $\%N_c$ of up to 0.3 g N 100 g^{-1} dry wt. For Belgium × Bintje, $\%N_c$ was not significantly different from Belgium × Charlotte (Fig. 6d).

There are two notable findings to point out. First, there were no significant differences between Minnesota × Russet Burbank and any other varieties evaluated in Minnesota or between Belgium × Bintje and Belgium × Charlotte. This finding did not hold true for all varieties within location evaluated, however; Significant differences between varieties were found for both Argentina and Canada. Second, the comparison between the Minnesota × Russet Burbank and Canada × Russet Burbank curves as well as the comparison between the Minnesota × Umatilla Russet and Argentina × Umatilla (Fig. S2) were both significantly different.

3.3.2. Differences related to statistical methods

When comparing the curves fit in the present study with the Bayesian hierarchical method to the curves fit in the previous studies using conventional statistical methods, there were significant differences between statistical curve fit methods for all varieties within location evaluated (Fig. 7). None of the previous CNDCs fall entirely within the credible region for the respective CNDCs developed in the present study.

The $\%N_c$ values from the previously developed CNDCs for the Argentina varieties (Giletto and Echeverría, 2015) were significantly less than that from the present CNDCs across all varieties for biomass levels of greater 5 Mg dry wt. ha^{-1} (Fig. 7). The magnitude of this difference was relatively large, with the $\Delta\%N_c$ between the previous and present method ranging up to –0.6 to –1.1 g N 100 g^{-1} dry wt., depending on variety. Therefore, relative to the statistical method used in this study it appears that the statistical methods used by Giletto and Echeverría (2015) selected biased critical points due to an overrepresentation of N limiting observations in the experimental dataset (Fig. 4, Fig. S1) leading to a systematic underestimation of $\%N_c$.

The $\%N_c$ from the previously developed CNDCs for Belgium (Ben Abdallah et al., 2016) were significantly greater than that from the CNDCs developed in the present study (Fig. 7). For all levels of biomass, $\Delta\%N_c$ between the previous and present methods was significantly different with a value of 0.7 g N 100 g^{-1} dry wt. Therefore, relative to the statistical method used in this study, it appears that the statistical methods used by Ben Abdallah et al. (2016) selected biased critical points due to overrepresentation of non-N limiting observations in the experimental dataset leading to a systematic overestimation of the $\%N_c$.

The $\%N_c$ from the previously developed CNDCs for Canada (Bélanger et al., 2001a) was significantly greater for both Canada × Russet Burbank and Canada × Shepody than the present CNDCs for biomass levels of less than 3 Mg dry wt ha^{-1} and greater than 6 Mg dry wt ha^{-1}, respectively (Fig. 7). Relative to the other locations, however, the CNDCs for Canada were the most similar between statistical methods, with a small value for $\Delta\%N_c$ of only 0.2 g N 100 g^{-1} dry wt. Therefore, relative to the statistical method used in this study, it appears that the statistical method used by Bélanger et al. (2001a) did not select biased critical points likely due to the lesser bias observed in this experimental dataset.

Because a CNDC using the conventional statistical methods has not been previously published for potato in Minnesota, no comparison across statistical methods is made for this experimental dataset. However, the bias observed in the Minnesota experimental dataset is similar to the bias found in the Belgium experimental dataset; therefore, using the conventional statistical methods to derive a CNDC for Minnesota would likely overestimat$\%N_c$ relative to the hierarchical Bayesian method.

4. Discussion

4.1. Mechanisms of dilution

While the present study presents direct evidence of significant differences between CNDCs for potato across G × E × M effects, previous studies help describe the potential physiological mechanisms for this source of variation. Reviewing previous work on this topic, Lemaire et al. (2019) described a framework with which to consider the variation in relative partitioning of dry matter. First, relative partitioning varies as biomass varies over the growing season indicating that there is an ontogentic relationship between harvest index and biomass. Second, the allometric trajectory of relative allocation (e.g., harvest index at a

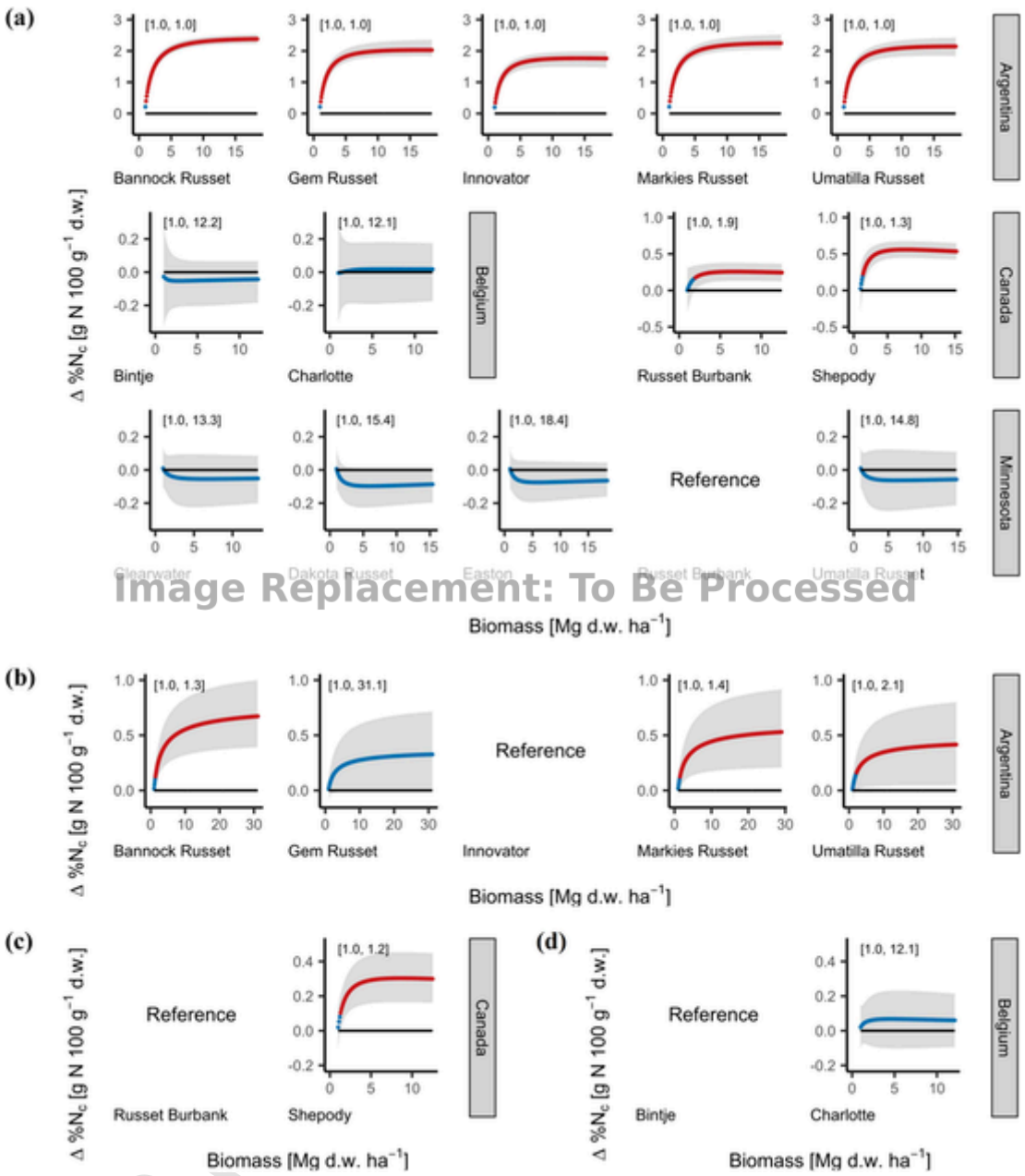

Fig. 6. Comparison of the difference in critical N concentration values [$\Delta\%N_c$] between (a) Minnesota × Russet Burbank and all other varieties within location, (b) Argentina × Innovator and all other varieties within Argentina, (c) Canada × Russet Burbank and all other varieties within Canada, and (d) Belgium × Bintje and all other varieties within Belgium. The grey shaded region represents the 90% credible region for $\Delta\%N_c$. The colored points represent the median value for $\Delta\%N_c$ at a given biomass level where blue or red color respectively indicates that the 90% credible region for $\Delta\%N_c$ does or does not contain zero. The solid black line at constant $\Delta\%N_c$ value of zero represents $\%N_c$ for the reference curve [$\%N_{c,ref}$] (i.e., Minnesota × Russet Burbank, Argentina × Innovator, Canada × Russet Burbank, and Belgium × Bintje). The range of biomass values for which $\Delta\%N_c$ is not significantly different (i.e., 90% credible region contains zero) is given in brackets.

given level of biomass) is subject to variation in non-ontogenetic factors (i.e., G × E × M interactions).

The findings of Giletto et al. (2020) suggest that the variation in CNDCs for potato are due to non-ontogenetic factors. In general, G × E × M interactions that result in greater and more rapid relative partitioning of biomass from vines (i.e., high N metabolic and structural tissue) to tubers (i.e., low N storage tissues) will result in greater N dilution (i.e., lower $\%N_c$) at the same level of total plant biomass (Lemaire et al., 2019). The two factors described by Giletto et al. (2020) affecting N dilution due to non-ontogenetic factors are total plant biomass at tuber initiation (i.e., timing of tuber initiation) and relative rate of tuber growth to plant growth (i.e., relative rate of tube bulking). These two factors are affected by various physiological mechanisms and G × E × M interactions; however, relatively limited work has been conducted to comprehensively evaluate the combined effect of G × E × M interaction on these two physiological mechanisms for potato.

4.1.1. *Timing of tuber initiation*

The timing of tuber initiation is affected primarily by variety maturity class (i.e., G). Potato varieties are classified on a spectrum of growth patterns where early maturing varieties are considered to be determinate and later maturing varieties are considered to be indeterminate (Thornton, 2020). Compared to indeterminate varieties, determinate varieties progress more quickly to the tuber initiation growth stage (i.e., at lower total plant biomass) and have a more rapid tuber bulking (i.e., biomass increase) with limited additional canopy and vine bio-

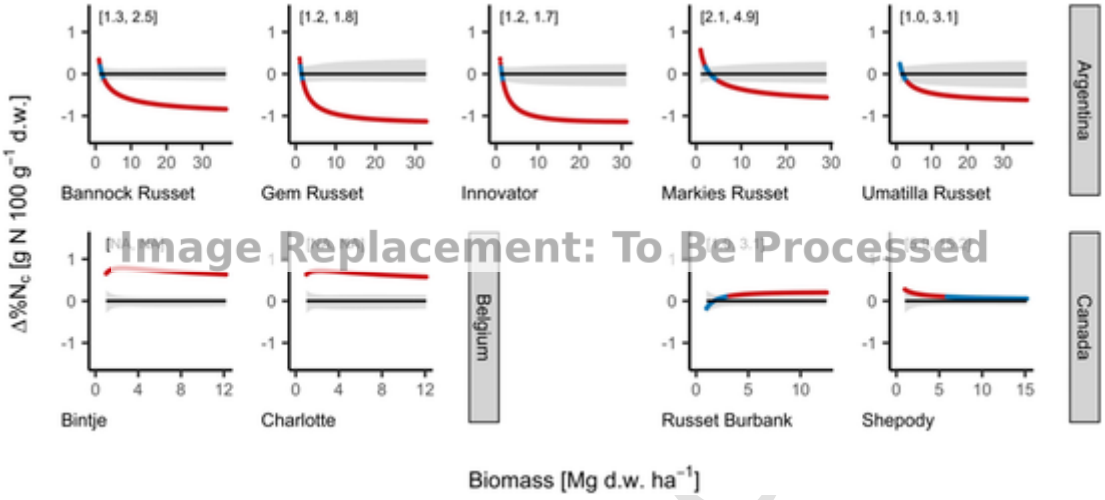

Fig. 7. Comparison of the difference in critical N concentration values [$\Delta\%N_c$] between the conventional statistical methods used in previous studies (i.e., Argentina – Giletto and Echeverría, 2015; Belgium – Ben Abdallah et al., 2016; Canada – Bélanger et al., 2001a) and the hierarchical Bayesian method used in the present study. The grey shaded region represents the 90% credible region for critical N concentration [$\%N_c$] using the directly modeled method. The solid black line at a constant $\Delta\%N_c$ value of zero represents the median value for $\%N_c$ using the directly modeled method. Red or blue points respectively indicate that $\Delta\%N_c$ falls outside of (i.e., is significant) or falls within (i.e., is not significant) the 90% credible region for $\%N_c$ determined by the directly modeled method. The range of biomass values for which Δ%Nc in not significant is given in brackets.

mass growth (i.e., increased harvest index for a given level of biomass) (Kleinkopf et al., 1981). Therefore, it is expected that increasing earliness of maturity for a potato variety would result in an increase in N dilution.

In the present study, differences in maturity class between varieties resulted in differences in $\%N_c$. For example, Argentina × Innovator, which has an early to medium maturity class, had significantly lower $\%N_c$ than Argentina × Bannock Russet, Argentina × Markies Russet, and Argentina × Umatilla Russet, which have either a medium-late to late or late to very late maturity class; however, Argentina × Gem Russet, which has a medium to late maturity class did not have a significantly different $\%N_c$ from Argentina × Innovator (Fig. S2). This finding supports the hypothesis that varieties with an earlier maturity class (i.e., earlier tuber initiation) will have lower $\%N_c$ (i.e., greater N dilution).

Timing of tuber initiation is also subject to G × E × M interactions. Ideal conditions for tuber initiation are moderate to low soil N availability, shorter day length, high light intensity, and cool nighttime temperatures (Ewing and Struik, 1992; Thornton, 2020); when N fertilizer management results in excessively high soil N availability (Kleinkopf et al., 1981), under conditions of reduced solar irradiance (Menzel, 1985), or when nighttime soil temperatures are elevated (Slater, 1968; Kim and Lee, 2019), tuber initiation can be delayed. Therefore, both M effects that result in excessive early-season soil N availability (e.g., all N applied at planting in a soluble form) and E effects that result in increased solar irradiance or reduced nighttime temperatures (i.e., increased diurnal temperature difference) could result in an increase in N dilution.

However, due the limitation of the experimental studies (i.e., the effect of M was not systematically varied across a given G × E interaction), it is not possible to directly assess the impact of diurnal temperature difference, solar irradiance, or N fertilizer source and timing (Table 3) on the timing of tuber initiation and N dilution distinct from the combined effect of G × E × M interactions.

4.1.2. Rate of tuber bulking

The rate of tuber bulking and allocation of biomass to tubers is subject to the effects of E. Conventionally, potential biomass production has been considered as the product of total solar radiation and radiation use efficiency (Monteith, 1977; Sinclair, 1999) as has been successfully applied to potato (Allen and Scott, 1980). Previous studies have suggested that decreasing diurnal temperature difference results in a reduction in tuber bulking rate (i.e., radiation use efficiency), most likely as a result of increasing utilization of photosynthesis assimilates for maintenance (via increased respiration) as nighttime temperature increases (Benoit et al., 1986; Bennett et al., 1991; Lizana et al., 2017); however, Kim and Lee (2019) did not observe any effect of increasing diurnal temperature difference on tuber bulking rate.

Given the limitation of the experimental studies (i.e., the effect of E was not systematically varied across a given G x M interaction), it is not possible to directly assess the impact of diurnal temperature difference and solar radiation (Table 3) on the rate of tuber bulking across G x E x M interactions.

Planting density is an important effect of M that may play a key role in determining the relative partitioning of biomass for to tuber. Previous studies investigating this effect have found that as planting density increases, leaf area index increases (Bremner and Taha, 1966; Ifenkwe and Allen, 1978; Allen and Scott, 1980), tuber dry weight biomass on a per area basis increases (Bremner and Taha, 1966; Ifenkwe and Allen, 1978), while tuber dry weight biomass on a per plant basis decreases (Bremner and Taha, 1966; Ifenkwe and Allen, 1978). The combination of the effect of increasing planting density could plausibly result in the net effect of an increased relative proportion of biomass allocated to vines (i.e., reduction in harvest index) (Vander Zaag et al., 1990), therefore reducing N dilution and resulting in an increased $\%N_c$.

In the present study, variations in $\%N_c$ due to variation in planting density were observed. For example, Argentina has the highest planting density of any location (Table 3) which resulted in greater $\%N_c$ than all other locations (Fig. S2). The relative effect of planting density also appears to be of greater magnitude than other sources of variation (e.g., maturity class). For example, Canada × Russet Burbank, which has a late to very late maturity class and planting density of 29,000 plants ha^{-1}, had a lower $\%N_c$ than Canada × Shepody, which has an early to medium-early maturity class and planting density of 44,000 plants ha^{-1} (Table 3, Fig. 6c). Therefore, this finding suggests that the effect of planting density (i.e., rate of tuber bulking) may be relatively more important at controlling $\%N_c$ than the effect of maturity class (i.e., timing of tuber initiation).

Because there was only a single level of M (e.g., planting density) within each level of G × E for the experimental trials considered here,

additional experimentation is required to fully consider the independent effects of G, E, and M on critical N dilution. Therefore, future experimental studies explicitly investigating the effect of M (e.g., planting density) on $\%N_c$ should be conducted to properly consider the combined effects the G × E × M interaction.

4.1.3. Comparison to other crops

These findings contrast somewhat with the previous studies evaluating G × E × M effects on $\%N_c$. Yao et al. (2021) found a similar magnitude of effect on $\%N_c$ for both G and E effects for wheat in China; however, Yao et al. (2021) also reported an E effect where $\%N_c$ for wheat in China was significantly different from that reported by Makowski et al. (2020) for wheat in France. Ciampitti et al. (2021) identified variation in $\%N_c$ for maize as a result of G × M interactions due to variation in hybrid and planting density. Fernández et al. (2021) found that variation in $\%N_c$ for tall fescue across G × E × M effects was negligible. In any case, the magnitude of the difference in $\%N_c$ across G × E × M interactions reported by the previous studies for wheat, maize, and tall fescue (Makowski et al., 2020; Ciampitti et al., 2021; Fernández et al., 2021; Yao et al., 2021) is less than that was observed in the present study for potato.

Therefore, the impact of G × E × M on $\%N_c$ is not only significant for potato, but is also of potentially of much greater relative importance compared to other crops (e.g., wheat, maize, tall fescue). This is because the magnitude of variability in $\%N_c$ due to G × E × M interactions found in the present study is relatively greater for potato than other crops; however, further additional experimental data are needed to confirm that this finding is not an artifact of the statistical methods or limitations of experimental data used in the present study.

4.1.4. Limitations of interpretation

Previous studies, including that of Giletto et al. (2020) on potatoes, have identified that N dilution follows a two-step process where the rate of N dilution varies between the vegetative period (i.e., parameter b_1) and the period of storage tissue accumulation (i.e., parameter b_2) (Duchenne et al., 1997; Plénet and Lemaire, 2000; Gastal et al., 2015). Our study, however, did not directly evaluate if the rate of N dilution during the pre-tuber initiation (i.e., vegetative growth) and post-tuber initiation (i.e., accumulation of storage tissue) periods varies due to G × E × M interactions. Variation in parameters b_1 and b_2 across G × E × M effects is a plausible physiological mechanism that could occur in addition to the non-ontogenetic allometric effects (i.e., timing of tuber initiation, relative rate of tube bulking) identified in the present study and used to explain variation in parameter b. This alternative hypothesis could be evaluated by modifying the Bayesian hierarchical method of the present study to include another hierarchical level representing the pre- and post-tuber initiation periods to determine if parameter b varies within these periods across to G × E × M interactions.

4.2. Implication of G × E variation on N use efficiency

Understanding and properly interpreting the impact of G × E × M effects on NUE is a critical goal necessary to improve N fertilizer use; however, this must be done while controlling for the effect of crop N status (Lemaire and Ciampitti, 2020). The previous findings of Bohman et al. (2021) demonstrated that interpreting NUE and its constituent component of N utilization efficiency [NUtE] is directly related to the parameters of the CNDC through the critical N utilization efficiency curve [CNUtEC] which defines the critical value of NUtE [$NUtE_c$]:

$$NUtE_c = 1000\left(10aW^{-b}\right)^{-1} \quad (11)$$

where parameters a and b, and W have the same meaning and units as previously defined in the present study and $NUtE_c$ has units of g dry wt. g^{-1} N. When NUtE is greater than $NUtE_c$, crop N status is deficient (i.e., NNI less than 1); conversely, when NUtE is less than $NUtE_c$, crop N status is excessive (i.e., NNI greater than 1).

The finding in the present study that the CNDC can vary across G × E × M interactions and the finding from Bohman et al. (2021) of the intrinsic relationship between NUE and the CNDC together lead to the conclusion that the CNUtEC must also vary across the same G × E × M effects as the CNDC. Therefore, the effect of G × E × M on variation of $NUtE_c$ is one of the multiple set of factors that ultimately control NUE. Understanding and accounting for the G × E × M effect on the CNUtEC is therefore critically important to understand the impacts of G × E × M interactions on NUE. In other words, controlling for this G × E × M effect represents an additional requirement when evaluating and interpreting NUE above and beyond the previously known requirements of controlling for both NNI and biomass (Barraclough et al., 2010; Caviglia et al., 2014; Sadras and Lemaire, 2014; Gastal et al., 2015; Lemaire and Ciampitti, 2020).

Following from the above discussion of the CNUtEC and the findings of Giletto et al. (2020), G × E × M effects that increase the relative proportion of biomass partitioned to tubers and reduce the time to tuber initiation will both decrease the $\%N_c$ and increase the $NUtE_c$ values. Therefore, future efforts to systematically improve NUE in potato through either management practices (e.g., Bohman et al., 2021) or crop breeding (e.g., Tiwari et al., 2018; Jones et al., 2021; Stefaniak et al., 2021) should focus on identifying G × E × M interactions that result in an increased proportion of biomass partitioned to tubers or result in earlier timing of tuber initiation.

4.3. Uncertainty in critical N concentration

4.3.1. Communicating uncertainty in critical N concentration

This study as well as others that implemented Bayesian statistical methods to derive critical N dilution curves (Makowski et al., 2020; Ciampitti et al., 2021; Yao et al., 2021) clearly indicate that there is meaningful uncertainty in $\%N_c$ values. Therefore, the use of $\%N_c$ in subsequent calculations should include this inherent uncertainty. However, the direct use of the credible region defined from posterior distribution of the fitted Bayesian hierarchical model in subsequent calculations is impractical, and a method to concisely and accurately communicate the credible region remains necessary.

Our finding that the credible region can be satisfactorily estimated using an equation of the same form as the CNDC (Fig. 5) suggests that an additional pair of negative exponential curves representing the upper and lower boundary of the credible region for $\%N_c$ (i.e., $CNDC_{lo}$ and $CNDC_{up}$) should be reported in future studies. In this manner, the median value and credible region for $\%N_c$ is defined by a set of three, two-parameter curves (i.e., CNDC – a, b; $CNDC_{up}$ – a_{up}, b_{up}; $CNDC_{lo}$ – a_{lo}, b_{lo}) which can be easily communicated and used in subsequent computations (Table 5).

4.3.2. Computing uncertainty of derived parameters

Critical N concentration and the associated CNDC parameters are commonly used to derive and calculate other related parameters. For example, the calculation of NNI depends on both $\%N_{Plant}$ and $\%N_{c,}$ (Eq. (1) and Eq. (2)). However, to properly account for the uncertainty in $\%N_c$ when computing NNI, the upper [$\%N_{c,up}$] and lower [$\%N_{c,lo}$] bounds of the credible interval for $\%N_c$ should also be used to determine the upper [NNI_{up}] and lower [NNI_{lo}] bounds of the credible interval for NNI, where $\%N_{c,up}$ and $\%N_{c,lo}$ are calculated using the $CNDC_{up}$ and $CNDC_{lo}$, respectively:

$$NNI_{up} = \%N_{Plant}/\%N_{c,up} = \%N_{Plant}/\left(a_{up}W_{up}^{-b}\right) \quad (12)$$

$$NNI_{lo} = \%N_{Plant}/\%N_{c,lo} = \%N_{Plant}/\left(a_{lo}W_{lo}^{-b}\right) \quad (13)$$

This has important practical implications for interpreting NNI values. For example, in a case where NNI is less than 1 but NNI_{up} is greater

than 1, it follows that crop N status would not be considered deficient (i.e., NNI is not significantly different from 1). In contrast, when both NNI and NNI_{lo} are greater than 1, it follows that crop N status would be considered surplus (i.e., NNI is significantly greater than 1). However, the threshold for considering significant differences in NNI will necessarily depend upon the threshold used for calculating $\%N_{c,lo}$ and $\%N_{c,up}$ (e.g., 90% confidence region). For example, the conclusions of a small-plot trial evaluating the effect of various N fertilizer treatments on yield and biomass (e.g., Bohman et al., 2021) may draw different conclusions when uncertainty in calculated NNI values is explicitly considered (e.g., N treatments were or were not limiting).

Additionally, the parameters of the CNDC (i.e., *a*, *b*) are also used to parameterize other related curves such as the critical N uptake curve [CNUC] or the critical N utilization efficiency curve [CNUtEC] (Bohman et al., 2021). When computing the critical N uptake [N_c] or critical N utilization efficiency [$NUtE_c$] values defined by these curves, respectively, the parameters from the $CNDC_{lo}$ (i.e., a_{lo}, b_{lo}) and $CNDC_{up}$ (i.e., a_{up}, b_{up}) should be used to calculate the upper and lower bounds of these derived values. In general, any calculation depending on either $\%N_c$ or any equation that uses the parameters of the CNDC, should also additionally use the $CNDC_{lo}$ and $CNDC_{up}$ to account for uncertainty in $\%N_c$.

4.4. Evaluating differences between statistical methods

While the occurrence of differences between CNDCs derived using the Bayesian hierarchical model compared to the conventional statistical methods (Fig. 6) is itself notable, the magnitude of the differences found in the present study is especially remarkable for the following reasons.

Because of its strong theoretical underpinning, $\%N_c$ and NNI are typically considered to be high fidelity measurements of crop N status, not affected by the subjectivity or relativity found in most other methods (Lemaire et al., 2019). However, the findings of the present study strongly suggest that this conception of the NNI framework must be qualified within a particular application by the statistical methods used to derive the CNDC for a given experimental dataset.

Unfortunately, the direct evaluation of different statistical methods to calculate the CNDC from the same experimental dataset cannot directly answer the question of which statistical method or resulting CNDC is "correct" (i.e., most accurate, least biased). However, we can reasonably conclude from both deduction and from the findings of the present study that a Bayesian hierarchical model utilizing the linear-plateau method and leveraging partial pooling across effect levels will result in inference that is less subjected to potential bias in the experimental data set compared to the conventional statistical methods. Additionally, it extracts the greatest amount of information from a given dataset, as no data are excluded from the fitting of the total model.

Therefore, it appears preferable for the future development of CNDCs to utilize the Bayesian hierarchical method to both quantify uncertainty and reduce bias in $\%N_c$. Without addressing these limitations (i.e., bias and uncertainty), both directly resulting from the statistical methods used, the NNI framework cannot fulfill its core objective of providing an absolute reference of crop N status.

Additionally, with further development of standardized tools for this scientific computing task, the implementation of the partially-pooled Bayesian hierarchical framework for deriving the CNDC can be made trivial and may enable the development of CNDCs from existing but unutilized experimental datasets. Therefore, the development of a dedicated software library to implement the partially-pooled Bayesian hierarchical method developed in the present study is a priority for future research efforts because it will enable other researchers to implement this preferred method of deriving CNDCs. This is of timely importance given the increased availability of high-quality, consolidated datasets suitable for fitting CNDCs across G × E × M effects (Ciampitti et al., 2022). Given the increased availability of data, future research should expand the partially-pooled Bayesian hierarchical method to fit models simultaneously using data from multiple crop species.

Finally, having sufficient quantity and quality of experimental data remains an essential criterion to consider when deriving a CNDC independent of the statistical method used (Fernández et al., 2021; Fernandez et al., 2022). Even with the advantages of the partially-pooled Bayesian hierarchical method, insufficient experimental data quality and quantity may still result in inferential bias of the CNDC for an individual G × E × M interaction level. Given the limitations of the quantity and quality of experimental data used in this study (i.e., bias towards N limiting conditions for Argentina, bias towards non-N limiting conditions for Belgium and Minnesota), it is plausible that estimates of CNDCs from this study are biased relative to estimates of CNDCs derived using an "ideal" experimental dataset and identical statistical methods. Therefore, future studies utilizing the partially-pooled Bayesian hierarchical method should ensure that the experimental dataset for each G × E × M interaction level meets the sufficiency criteria identified by Fernández et al. (2022) (i.e., at least eight experimental trials containing at least three N treatments and at least three sampling dates).

5. Conclusions

First, this study demonstrated that there are significant differences between CNDCs developed across G × E × M effects for potato. Therefore, any application of $\%N_c$ must use an appropriate CNDC (i.e., not significantly different) for the G × E × M interaction being considered. Second, this study developed an approach to communicate uncertainty in $\%N_c$ through the concise set of six parameters defined by the CNDC (i.e., *a*, *b*), $CNDC_{lo}$ (i.e., a_{lo}, b_{lo}), and $CNDC_{up}$ (i.e., a_{up}, b_{up}), and the $\%N_c$ value computed from these three curves should be used in all subsequent computations to propagate uncertainty. Third, this study demonstrated that the statistical method used to derive CNDCs affects the inferred $\%N_c$ values, and that the partially-pooled hierarchical Bayesian framework is less susceptible to bias due to insufficient quantity and quality of experimental data than the conventional statistical methods. Therefore, future efforts to derive CNDCs should utilize the partially-pooled hierarchical Bayesian framework whenever possible. Fourth, the findings of this study suggest that variation in $\%N_c$ across G × E × M interactions necessarily extends to NUE, via the relationship between the CNDC and the CNUtEC. Therefore, NUE is dependent on the mechanisms that control N dilution (i.e., biomass partitioning), and future efforts to improve NUE should explicitly consider how G × E × M interactions affect N dilution.

Uncited references

; .

CRediT authorship contribution statement

Brian J. Bohman : Writing – original draft, Formal analysis, Data curation, Visualization, Investigation, Conceptualization, Methodology, Software. **Michael J. Culshaw-Maurer :** Writing – original draft, Methodology, Software, Formal analysis, Visualization. **Feriel Ben Abdallah :** Writing – review & editing, Investigation, Data curation. **Claudia Giletto :** Writing – review & editing, Investigation, Data curation. **BelangerGilles Bélanger :** Writing – review & editing, Investigation, Data curation. **FernandezFabián G. Fernández :** Writing – review & editing, Supervision. **Yuxin Miao :** Writing – review & editing, Supervision. **David J. Mulla :** Writing – review & editing, Supervision. **Carl J. Rosen :** Writing – review & editing, Project administration, Funding acquisition, Supervision, Investigation, Methodology, Data curation, Resources.

Declaration of Competing Interest

The authors declare the following financial interests/personal relationships which may be considered as potential competing interests: Carl J. Rosen reports financial support was provided by Minnesota Area II Potato Growers Research and Promotion Council.

Data Availability

The entire statistical and data workflow used for this manuscript is reproducible and available via GitHub repository (https://github.com/bohm0072/bayesian-cndc-potato).

Acknowledgements

Research funding for this project was provided by Minnesota Area II Potato Growers Research and Promotion Council..

Appendix A. Supporting information

Supplementary data associated with this article can be found in the online version at doi:10.1016/j.eja.2023.126744.

References

Allen, E.J., Scott, R.K., 1980. An analysis of growth of the potato crop. J. Agr. Sci. 94 (3), 583–606. https://doi.org/10.1017/S0021859600028598.

CFIA. 2013. Bintje: Canadian Food Inspection Agency. Retrieved from ⟨https://inspection.canada.ca/plant-varieties/potatoes/potato-varieties/bintje/eng/1312587385655/1312587385656⟩.

USDA NRCS. 2013. Soil Series Classification Database – Hubbard Series: United States Department of Agriculture. Retrieved from ⟨https://soilseries.sc.egov.usda.gov/OSD_Docs/H/HUBBARD.html⟩.

AHDB. 2015. Charlotte: Agriculture and Horticulture Development Board. Retrieved from ⟨https://varieties.ahdb.org.uk/varieties/view/CHARLOTTE⟩.

Weather Spark. 2021. Compare the Climate and Weather in Becker, Saint-Léonard, Balcarce, and Gembloux. Retrieved from ⟨https://weatherspark.com/compare/y/10443–27617~28950–51092/Comparison-of-the-Average-Weather-in-Becker-Saint-L%C3%A9onard-Balcarce-and-Gembloux⟩.

Barraclough, P.B., Howarth, J.R., Jones, J., Lopez-Bellido, R., Parmar, S., Shepherd, C.E., Hawkesford, M.J., 2010. Nitrogen efficiency of wheat: genotypic and environmental variation and prospects for improvement. Eur. J. Agron. 33 (1), 1–11. https://doi.org/10.1016/j.eja.2010.01.005.

OSU. 2021. Potato Variety Identification and Ownership Table: Oregon State University – Oregon Seed Certification Service. Retrieved from ⟨https://seedcert.oregonstate.edu/sites/seedcert.oregonstate.edu/files/potato_varietyratingkey.pdf⟩.

Bates, D.M. 2010. *Lme4: Mixed-Effects Modeling with R*.

Bélanger, G., Walsh, J.R., Richards, J.E., Milburn, P.H., Ziadi, N., 2000. Yield response of two potato culivars to supplemental irrigation and N fertilization in new brunswick. Am. J. Potato Res. 77 (1), 11–21. https://doi.org/10.1007/BF02853657.

Bélanger, G., Walsh, J.R., Richards, J.E., Milburn, P.H., Ziadi, N., 2001a. Critical nitrogen curve and nitrogen nutrition index for potato in eastern Canada. Am. J. Potato Res 78 (5), 355–364. https://doi.org/10.1007/BF02884344.

Bélanger, G., Walsh, J.R., Richards, J.E., Milburn, P.H., Ziadi, N., 2001b. Tuber growth and biomass partitioning of two potato cultivars grown under different N fertilization rates with and without irrigation. Am. J. Potato Res. 78 (2), 109–117. https://doi.org/10.1007/BF02874766.

Ben Abdallah, F., Olivier, M., Goffart, J.P., Minet, O., 2016. Establishing the nitrogen dilution curve for potato cultivar bintje in Belgium. Potato Res. 59 (3), 241–258. https://doi.org/10.1007/s11540-016-9331-y.

Bennett, S.M., Tibbitts, T.W., Cao, W., 1991. Diurnal temperature fluctuation effects on potatoes grown with 12 hr photoperiods. Am. Potato J. 68, 81–86. https://doi.org/10.1007/BF02853925.

Benoit, G.R., Grant, W.J., Devine, O.J., 1986. Potato top growth as influenced by day-night temperature differences. Agron. J. 78 (2), 264–269. https://doi.org/10.2134/agronj1986.00021962007800020010x.

Bohman, B.J., M. McNearney, J. Crants, and C.J. Rosen. 2020. A Novel Approach to Manage Nitrogen Fertilizer for Potato Production Using Remote Sensing. Research Reports – 2020. Fargo, ND: Minnesota Area II Potato Research and Promotion Council and Northern Plains Potato Growers Association. Retrieved from ⟨https://www.ag.ndsu.edu/potatoextension/research/2020ResearchBooks.pdf⟩.

Bohman, B.J., Rosen, C.J., Mulla, D.J., 2021. Relating nitrogen use efficiency to nitrogen nutrition index for evaluation of agronomic and environmental outcomes in potato. Field Crops Res. 262. https://doi.org/10.1016/j.fcr.2020.108041.

Bremner, P.M., Taha, M.A., 1966. Studies in potato agronomy. I. The effects of variety, seed size and spacing on growth, development and yield. J. Agric. Sci. 66 (2), 241–252. https://doi.org/10.1017/s0021859600062651.

Bürkner, P.-C., 2017. brms: an R package for bayesian multilevel models using stan. J. Stat. Softw. 80 (1). https://doi.org/10.18637/jss.v080.i01.

Bürkner, P.-C., 2018. Advanced bayesian multilevel modeling with the R package brms. R. J. 10 (1), 395–411. https://doi.org/10.32614/RJ-2018-017.

Carpenter, B., Gelman, A., Hoffman, M.D., Lee, D., Goodrich, B., Betancourt, M., Brubaker, M., Guo, J., Li, P., Riddell, A., 2017. Stan: a probabilistic programming language. J. Stat. Softw. 76 (1). https://doi.org/10.18637/jss.v076.i01.

Caviglia, O.P., Melchiori, R.J.M., Sadras, V.O., 2014. Nitrogen utilization efficiency in maize as affected by hybrid and N rate in late-sown crops. Field Crops Res. 168, 27–37. https://doi.org/10.1016/j.fcr.2014.08.005.

Ciampitti, I., van Versendaal, E., Rybecky, J.F., Lacasa, J., Fernandez, J., Makowski, D., Lemaire, G., 2022. A global dataset to parametrize critical nitrogen dilution curves for major crop species. Sci. Data 9 (1), 277. https://doi.org/10.1038/s41597-022-01395-2.

Ciampitti, I.A., Fernandez, J., Tamagno, S., Zhao, B., Lemaire, G., Makowski, D., 2021. Does the critical N dilution curve for maize crop vary across genotype X environment x management scenarios? - a bayesian analysis. Eur. J. Agron. 123, 126202. https://doi.org/10.1016/j.eja.2020.126202.

R. Core Team. (2021b). "Stats": The R Stats Package. Retrieved from ⟨https://CRAN.R-project.org/package=stats⟩.

Core Team, R., 2021a. R: A Language and Environment for Statistical Computing. R Foundation for Statistical Computing, Vienna, Austria. ⟨https://www.R-project.org/⟩.

Crants, J., C. Rosen, M. McNearney, and L. Sun. 2017. The Use of Chlorophyll Meters for Nitrogen Management in Potatoes. Research Reports – 2017. Fargo, ND: Minnesota Area II Potato Research and Promotion Council and Northern Plains Potato Growers Association. Retrieved from ⟨https://www.ag.ndsu.edu/potatoextension/research⟩.

Duchenne, T., Machet, J.M., Martin, M., 1997. Potatoes. In: Lemaire, G. (Ed.), Diagonsis of the Nitrogen Status in Crops. Springer, Berlin, pp. 119–130.

Egel, D.S. 2017. Midwest Vegetable Production Guide for Commercial Growers. *BU-07094-S*: University of Minnesota Extension. Retrieved from ⟨https://ag.purdue.edu/btny/midwest-vegetable-guide/Pages/default.aspx⟩.

Errebhi, M., Rosen, C.J., Gupta, S.C., Birong, D.E., 1998. Potato yield response and nitrate leaching as influenced by nitrogen management. Agron. J. 90, 10–15. https://doi.org/10.2134/agronj1998.00021962009000010003x.

Ewing, E.E., Struik, P.C., 1992. Tuber formation in potato: induction, initiation, and growth. In: Janick, J. (Ed.)Horticultural Reviews, Volume 14. John Wiley & Sons, pp. 89–198.

Fernandez, J.A., van Versendaal, E., Lacasa, J., Makowski, D., Lemaire, G., Ciampitti, I.A., 2022. Dataset characteristics for the determination of critical nitrogen dilution curves: from past to new guidelines. Eur. J. Agron. 139, 126568. https://doi.org/10.1016/j.eja.2022.126568.

Fernández, J.A., Lemaire, G., Bélanger, G., Gastal, F., Makowski, D., Ciampitti, I.A., 2021. Revisiting the critical nitrogen dilution curve for tall fescue: a quantitative synthesis. Eur. J. Agron. 131, 126380. https://doi.org/10.1016/j.eja.2021.126380.

Franzen, D., A. Robinson, and C. Rosen. 2018. Fertilizing Potato in North Dakota. SF715. Fargo, ND: North Dakota State University. Retrieved from ⟨https://www.ag.ndsu.edu/publications/crops/fertilizing-potato-in-north-dakota⟩.

Gastal, F., Lemaire, G., Durand, J.-L., 2015. Quantifying Crop Responses to Nitrogen and Avenues to Improve Nitrogen-Use Efficiency. In: Crop Physiology. Second ed., pp. 161–206. https://doi.org/10.1016/b978-0-12-417104-6.00008-x.

Gelaro, R., McCarty, W., Suarez, M.J., Todling, R., Molod, A., Takacs, L., Randles, C., Darmenov, A., Bosilovich, M.G., Reichle, R., Wargan, K., Coy, L., Cullather, R., Draper, C., Akella, S., Buchard, V., Conaty, A., da Silva, A., Gu, W., Kim, G.K., Koster, R., Lucchesi, R., Merkova, D., Nielsen, J.E., Partyka, G., Pawson, S., Putman, W., Rienecker, M., Schubert, S.D., Sienkiewicz, M., Zhao, B., 2017. The modern-era retrospective analysis for research and applications, version 2 (Merra-2). J. Clim. Volume 30 (Iss 13), 5419–5454. https://doi.org/10.1175/JCLI-D-16-0758.1.

Giletto, C.M., Echeverría, H.E., 2015. Critical nitrogen dilution curve in processing potato cultivars. Am. J. Plant Sci. 6 (19), 3144–3156. https://doi.org/10.4236/ajps.2015.619306.

Giletto, C.M., Reussi Calvo, N.I., Sandaña, P., Echeverría, H.E., Bélanger, G., 2020. Shoot- and tuber-based critical nitrogen dilution curves for the prediction of the N status in potato. Eur. J. Agron. 119. https://doi.org/10.1016/j.eja.2020.126114.

Greenwood, D.J., Neeteson, J.J., Draycott, A., 1986. Quantitative relationships for the dependence of growth rate of arable crops on their nitrogen content, dry weight and aerial environment. Plant Soil 91 (3), 281–301. https://doi.org/10.1007/BF02198111.

Greenwood, D.J., Lemaire, G., Gosse, G., Cruz, P., Draycott, A., Neeteson, J.J., 1990. Decline in percentage N of C3 and C4 crops with increasing plant mass. Ann. Bot. 66 (4), 425–436. https://doi.org/10.1093/oxfordjournals.aob.a088044.

Gupta, S., and C.J. Rosen. 2019. Nitrogen Fertilization Rate and Cold-Induced Sweetening in Potato Tubers During Storage. Research Reports – 2019. Fargo, ND: Minnesota Area II Potato Research and Promotion Council and Northern Plains Potato Growers Association. Retrieved from ⟨https://www.ag.ndsu.edu/potatoextension/research/2019RESEARCHREPORTS.pdf⟩.

Gupta, S.K., J. Crants, M. McNearney, and C.J. Rosen. 2020. Evaluation of a Promising Minnesota Clone for N Response, Agronomic Traits & Storage Quality. Research Reports – 2020. Fargo, ND: Minnesota Area II Potato Research and Promotion Council and Northern Plains Potato Growers Association. Retrieved from ⟨https://www.ag.ndsu.edu/potatoextension/research/2020ResearchBooks.pdf⟩.

Hansen, B., 1988. Sand Plains Research Farm Soil Report. University of Minnesota, St. Paul, MN.

Herrmann, A., Taube, F., 2004. The range of the critical nitrogen dilution curve for maize (Zea mays L.) can be extended until silage maturity. Agron. J. 96 (4), 1131–1138. https://doi.org/10.2134/agronj2004.1131.

Horneck, D.A., Miller, R.O., 1998. Determination of total nitrogen in plant tissue. In: Kalra, Y.P. (Ed.), Handbook of Reference Methods for Plant Analysis. CRC Press,

Boston, pp. 75–84.
Horwitz, W., Chichilo, P., Reynolds, H., 1970. Official Methods of Analysis of the Association of Official Analytical Chemists, 11th ed..,. Association of Official Analytical Chemists, Washington, DC.
Houlès, V., Guérif, M., Mary, B., 2007. Elaboration of a nitrogen nutrition indicator for winter wheat based on leaf area index and chlorophyll content for making nitrogen recommendations. Eur. J. Agron. 27 (1), 1–11. https://doi.org/10.1016/j.eja.2006.10.001.
Ifenkwe, O.P., Allen, E.J., 1978. Effects of row width and planting density on growth and yield of two maincrop potato varieties. 1. Plant morphology and dry-matter accumulation. J. Agric. Sci. 91 (2), 265–278. https://doi.org/10.1017/s0021859600046359.
Jones, C.R., Michaels, T.E., Carley, C.S., Rosen, C.J., Shannon, L.M., 2021. Nitrogen uptake and utilization in advanced fresh-market red potato breeding lines. Crop Sci. 61, 878–895. https://doi.org/10.1002/csc2.20297.
Justes, E., Mary, B., Meynard, J.-M., Machet, J.-M., Thelier-Huche, L., 1994. Determination of a critical nitrogen dilution curve for winter wheat crops. Ann. Bot. 74 (4), 397–407. https://doi.org/10.1006/anbo.1994.1133.
Kim, Y.U., Lee, B.W., 2019. Differential mechanisms of potato yield loss induced by high day and night temperatures during tuber initiation and bulking: photosynthesis and tuber growth. Front. Plant Sci. 10, 300. https://doi.org/10.3389/fpls.2019.00300.
Kleinkopf, G.E., Westermann, D.T., Dwelle, R.B., 1981. Dry matter production and nitrogen utilization by six potato cultivars. Agron. J. 73 (5), 799–802. https://doi.org/10.2134/agronj1981.00021962007300050013x.
Lemaire, G., Ciampitti, I., 2020. Crop mass and N status as prerequisite covariables for unraveling nitrogen use efficiency across genotype-by-environment-by-management scenarios: a review. Plants 9 (10). https://doi.org/10.3390/plants9101309.
Lemaire, G., Gastal, F., 1997. N uptake and distribution in plant canopies. In: Lemaire, G. (Ed.), Diagnosis of the Nitrogen Status in Crops. Springer, Berlin, pp. 3–43.
Lemaire, G., Sinclair, T., Sadras, V., Bélanger, G., 2019. Allometric approach to crop nutrition and implications for crop diagnosis and phenotyping. A review. Agron. Sustain. Dev. 39 (2). https://doi.org/10.1007/s13593-019-0570-6.
Li, D., Miao, Y., Gupta, S.K., Rosen, C.J., Yuan, F., Wang, C., Wang, L., Huang, Y., 2021. Improving potato yield prediction by combining cultivar information and uav remote sensing data using machine learning. Remote Sens. 13 (16). https://doi.org/10.3390/rs13163322.
Lindstrom, M.J., Bates, D.M., 1990. Nonlinear mixed effects models for repeated measures data. Biometrics 46 (3), 673–687. https://doi.org/10.2307/2532087.
Lizana, X.C., Avila, A., Tolaba, A., Martinez, J.P., 2017. Field responses of potato to increased temperature during tuber bulking: projection for climate change scenarios, at high-yield environments of southern chile. Agric. . Meteorol. 239, 192–201. https://doi.org/10.1016/j.agrformet.2017.03.012.
Makowski, D., Zhao, B., Ata-Ul-Karim, S.T., Lemaire, G., 2020. Analyzing uncertainty in critical nitrogen dilution curves. Eur. J. Agron. 118. https://doi.org/10.1016/j.eja.2020.126076.
McElreath, R., 2020. Staistical Rethinking: A Bayesian Course with Examples in R and Stan, second ed. Chapman and Hall/CRC, Boca Raton.
Menzel, C.M., 1985. Tuberization in potato at high temperatures: interaction between temperature and irradiance. Ann. Bot. 55 (1), 35–39. https://doi.org/10.1093/oxfordjournals.aob.a086875.
Monteith, J.L., 1977. Climate and the efficiency of crop production in Britain. Philos. Trans. R. Soc. Lond. B 281, 277–294. https://doi.org/10.1098/rstb.1977.0140.
Morier, T., Cambouris, A.N., Chokmani, K., 2015. In-season nitrogen status assessment and yield estimation using hyperspectral vegetation indices in a potato crop. Agron. J. 107 (4), 1295–1309. https://doi.org/10.2134/agronj14.0402.
Morris, T.F., Murrell, T.S., Beegle, D.B., Camberato, J.J., Ferguson, R.B., Grove, J., Ketterings, Q., Kyveryga, P.M., Laboski, C.A.M., McGrath, J.M., Meisinger, J.J., Melkonian, J., Moebius-Clune, B.N., Nafziger, E.D., Osmond, D., Sawyer, J.E., Scharf, P.C., Smith, W., Spargo, J.T., van Es, H.M., Yang, H., 2018. Strengths and limitations of nitrogen rate recommendations for corn and opportunities for improvement. Agron. J. 110 (1), 1. https://doi.org/10.2134/agronj2017.02.0112.
Plénet, D., Lemaire, G., 2000. Relationships between dynamics of nitrogen uptake and dry matter accumulation in maize crops. Determination of critical N concentration. Plant Soil 216 (1/2), 65–82. https://doi.org/10.1023/a:1004783431055.
Plummer, M. 2013. jags: Just Another Gibs Sampler. Retrieved from ⟨http://mcmc-jags.sourceforge.net/⟩.
Plummer, M. 2019. Rjags: Bayesian Graphical Models Using Mcmc. Retrieved from ⟨https://CRAN.R-project.org/package=rjags⟩.
Porter, G. 2014. 201400091. USDA PVPO.
Rosen, C., D. Birong, and M. Zumwinkle. 1992. Nitrogen Fertilization Studies on Irrigated Potatoes: Nitrogen Use, Soil Nitrate Movement, and Petiole Sap Nitrate Analysis for Predicting Nitrogen Needs. *Field Research in Soil Science – Soil Series #134*. St. Paul, MN: University of Minnesota. Retrieved from ⟨https://conservancy.umn.edu/handle/11299/121705⟩.
Rosen, C., M. Errebhi, J. Moncrief, S. Gupta, H.H. Cheng, and D. Birong. 1993. Nitrogen Fertilization Studies on Irrigated Potatoes: Nitrogen Use, Soil Nitrate Movement, and Petiole Sap Nitrate Analysis for Predicting Nitrogen Needs. Field Research in Soil Science – Soil Series #136. St. Paul, MN: University of Minnesota. Retrieved from ⟨https://conservancy.umn.edu/handle/11299/121706⟩.
Rosen, C., J. Crants, B. Bohman, and M. McNearney. 2021. Effects of Banded Versus Broadcast Application of ESN, Turkey Manure, and Different Approaches to Measuring Plant N Status on Tuber Yield and Quality in Russet Burbank Potatoes. Reserach Reports – 2021. Fargo, ND: Minnesota Area II Potato Research and Promotion Council and Northern Plains Potato Growers Association. Retrieved from ⟨https://www.ag.ndsu.edu/potatoextension/research/research_reports_114_4126022392.pdf⟩.
Rosen, C.J. 2018. Potato Fertilization on Irrigated Soils: University of Minnesota Extension. Retrieved from ⟨https://extension.umn.edu/crop-specific-needs/potato-fertilization-irrigated-soils⟩.
Sadras, V.O., Lemaire, G., 2014. Quantifying crop nitrogen status for comparisons of agronomic practices and genotypes. Field Crops Res. 164, 54–64. https://doi.org/10.1016/j.fcr.2014.05.006.
Schad, D.J., Betancourt, M., Vasishth, S., 2021. Toward a principled bayesian workflow in cognitive science. Psychol. Methods 26 (1), 103–126. https://doi.org/10.1037/met0000275.
USDA. 1997. United States Standards for Grades of Potatoes for Processing. Retrieved from ⟨https://www.ams.usda.gov/sites/default/files/media/Potatoes_for_Processing_Standard%5B1%5D.pdf⟩.
Slater, J.W., 1968. The effect of night temperature on tuber initiation of the potato. Eur. Potato J. 11 (1), 14–22. https://doi.org/10.1007/BF02365158.
Sinclair, T.R., and R.C. Muchow. 1999. Radiation Use Efficiency. In D. L. Sparks (Ed.), Advances in Agronomy, Volume 65 (Vol. 65, pp. 215–265).doi:10.1016/S0065-2113(08)60914-1
Stark, J.C., Thompson, A.L., Novy, R., 2020. Variety Selection and Management. In: Stark, J. C., Thornton, M., Nolte, P. (Eds.), Potato Production Systems. pp. 35–64.
Steele, D.D., Scherer, T.F., Wright, J., Hopkins, D.G., Tuscherer, S.R., Wright, J., 2010. Spreadsheet implementation of irrigation scheduling by the checkbook method for North Dakota and Minnesota. Appl. Eng. Agric. 26, 983–996. https://doi.org/10.13031/2013.35914.
Stefaniak, T.R., Fitzcollins, S., Figueroa, R., Thompson, A.L., Schmitz Carley, C., Shannon, L.M., 2021. Genotype and variable nitrogen effects on tuber yield and quality for red fresh market potatoes in Minnesota. Agronomy 11, 255. https://doi.org/10.3390/agronomy11020255.
Sun, N. 2017. Agronomic and Storage Factors Affecting Acrylamide Formation in Processed Potatoes. (Ph.D.). University of Minnesota, St. Paul, MN. Retrieved from ⟨https://conservancy.umn.edu/handle/11299/190488⟩.
Sun, N., Wang, Y., Gupta, S.K., Rosen, C.J., 2019. Nitrogen fertility and cultivar effects on potato agronomic properties and acrylamide-forming potential. Agron. J. 111 (1), 408. https://doi.org/10.2134/agronj2018.05.0350.
Sun, N., Wang, Y., Gupta, S.K., Rosen, C.J., 2020. Potato tuber chemical properties in storage as affected by cultivar and nitrogen rate: implications for acrylamide formation. Foods 9 (3). https://doi.org/10.3390/foods9030352.
Thompson, A. 2013. 201300475. USDA PVPO.
Thornton, M., 2020. Potato growth and development. In: Stark, J.C., Thornton, M., Nolte, P. (Eds.), Potato Production Systems. pp. 19–33.
Tiwari, J.K., Plett, D., Garnett, T., Chakrabarti, S.K., Singh, R.K., 2018. Integrated genomics, physiology and breeding approaches for improving nitrogen use efficiency in potato: translating knowledge from other crops. Funct. Plant Biol. 45 (6), 587. https://doi.org/10.1071/fp17303.
Ushey, K. 2021. renv: Project Environments. Retrieved from ⟨https://CRAN.R-project.org/package=renv⟩.
Vander Zaag, P., Demagante, A.L., Ewing, E.E., 1990. Influence of plant spacing on potato (Solanum tuberosum L.) morphology, growth and yield under two contrasting environments. Potato Res. 33 (313–323). https://doi.org/10.1007/BF02359305.
Vehtari, A., Gelman, A., Simpson, D., Carpenter, B., Bürkner, P.-C., 2021. Rank-normalization, folding, and localization: an improved R-hat for assessing convergence of MCMC (with Discussion). Bayesian Anal. 16 (2), 667–718. https://doi.org/10.1214/20-BA1221.
Wright, J. 2002. Irrigation Scheduling Checkbook Method. BU-FO-01322. St. Paul, MN: University of Minnesota. Retrieved from ⟨https://extension.umn.edu/irrigation/irrigation-scheduling-checkbook-method⟩.
Yao, B., Wang, X., Lemaire, G., Makowski, D., Cao, Q., Liu, X., Liu, L., Liu, B., Zhu, Y., Cao, W., Tang, L., 2021. Uncertainty analysis of critical nitrogen dilution curves for wheat. Eur. J. Agron. 128, 126315. https://doi.org/10.1016/j.eja.2021.126315.